

INDUCED-GRAVITY GUT-SCALE HIGGS INFLATION IN SUPERGRAVITY

CONSTANTINOS PALLIS¹ AND QAISAR SHAFI²

¹*School of Electrical & Computer Engineering, Faculty of Engineering,
Aristotle University of Thessaloniki, GR-541 24 Thessaloniki, GREECE*
e-mail address: kpallis@gen.auth.gr

²*Bartol Research Institute, Department of Physics and Astronomy,
University of Delaware, Newark, DE 19716, USA*
e-mail address: shafi@bartol.udel.edu

ABSTRACT: Models of induced-gravity inflation are formulated within Supergravity employing as inflaton the Higgs field which leads to a spontaneous breaking of a $U(1)_{B-L}$ symmetry at $M_{\text{GUT}} = 2 \cdot 10^{16}$ GeV. We use a renormalizable superpotential, fixed by a $U(1)$ R symmetry, and Kähler potentials which exhibit a prominent shift-symmetric part and a tiny violation included in a logarithm with prefactor $-(2n+3)$ or $-2(1+n)$. We find inflationary solutions of Starobinsky type for $-0.06 \lesssim n \lesssim 0.051$ and others (more marginal) which resemble those of linear inflation for $-0.32 \lesssim n \lesssim -0.15$. In both cases the inflaton mass is predicted to be of the order of 10^{13} GeV. Extending the superpotential of the model with suitable terms we show how the MSSM μ parameter can be generated. Also, non-thermal leptogenesis can be successfully realized, provided that the gravitino is heavier than about 10 TeV.

PACs numbers: 98.80.Cq, 04.50.Kd, 12.60.Jv, 04.65.+e

I. INTRODUCTION

The idea of *induced gravity* (IG), according to which the (reduced) Planck mass m_{P} is generated [1] via the *vacuum expectation value* (v.e.v) that a scalar field acquires at the end of a phase transition in the early universe, has recently attracted a fair amount of attention. This is because it may follow an inflationary stage driven by a Starobinsky-type potential [2] in *Supergravity* (SUGRA) [3–7] and in non-*Supersymmetric* (SUSY) [8–12] settings, which turns out to be nicely compatible with the observational data [13]. As a bonus, the resulting effective theories do not suffer from any problem with perturbative unitarity [3, 5, 11, 14, 15] in sharp contrast to some models of non-minimal inflation [16–19] where the inflaton after inflation assumes a v.e.v much smaller than m_{P} .

The simplest way to realize the idea of IG is to employ a double-well potential, $\lambda(\phi^2 - v^2)^2$, for the inflaton ϕ [1, 3–5, 8–11] – scale invariant realizations of this idea are proposed in Ref. [12]. If we adopt a non-minimal coupling to gravity [9, 10] of the type $f_{\mathcal{R}} = c_{\mathcal{R}}\phi^2$ and set $v = m_{\text{P}}/\sqrt{c_{\mathcal{R}}}$, then $\langle f_{\mathcal{R}} \rangle = m_{\text{P}}^2$, i.e., $f_{\mathcal{R}}$ reduces to m_{P}^2 at the vacuum generating, thereby, Einstein gravity at low energies. The implementation of inflation, on the other hand, which requires the emergence of a sufficiently flat branch of the potential at large field values constrains $c_{\mathcal{R}}$ to sufficiently large values and λ as a function of $c_{\mathcal{R}}$. An even more restrictive version of this scenario would be achieved if ϕ is involved in a Higgs sector which triggers a *Grand Unified Theory* (GUT) phase transition in the early Universe [7, 9]. The scale of a such transition is usually related to the (field dependent) mass of the lightest gauge boson and can be linked to some unification condition in *supersymmetric* (SUSY) – most notably – settings [19–23]. As a consequence, $c_{\mathcal{R}}$ can be uniquely determined by the theoretical requirements, giving rise to an economical, predictive and well-motivated set-up, thereby called *IG Higgs inflation* (IGHI). To our knowledge, the unification hypothesis has not been previously employed in constraining IGHl.

Since gauge coupling unification is elegantly achieved

within the *minimal supersymmetric standard model* (MSSM), we need to formulate IGHl in the context of SUGRA. We rely here on the models of kinetically modified non-minimal *Higgs inflation* (HI) established in Ref. [20–23]. We employ there a renormalizable superpotential, uniquely determined by a gauge and a $U(1)$ R symmetry, which realizes the Higgs mechanism in a SUSY framework. Actually, this is the same superpotential widely used for the models of F-term hybrid inflation [24–28]. Contrary to that case, though, where the inflaton typically is a gauge singlet and a pair of gauge non-singlets are stabilized at zero, here the inflaton is involved in the Higgs sector of the theory whereas the gauge singlet superfield is confined at the origin playing the role of a *stabilizer* – for a related scenario see Ref. [29]. As regards the Kähler potentials, we concentrate on semi-logarithmic ones which exhibit a softly broken shift symmetry [20, 30, 31], employ variable coefficients for the logarithmic part and include only quadratic terms of the various fields, taking advantage of the recently established [6] stabilization mechanisms of the accompanying non-inflaton fields. The term “kinetically modified” associated with such models is introduced in Ref. [21, 32] since, apart from the non-minimal coupling to gravity $f_{\mathcal{R}} = 1 + c_+\phi^2$, these models exhibit a kinetic mixing of the form $f_{\mathcal{K}} \simeq c_-f_{\mathcal{R}}$, where the constants c_- and c_+ can be interpreted as the coefficients of the principal shift-symmetric term (c_-) and its violation (c_+) in the Kähler potentials. The observables depend on the ratio $r_{\pm} = c_+/c_-$, and excellent agreement with the recent data [13, 33] can be achieved.

Kinetically modified non-minimal HI can be easily promoted to GUT-scale IGHl if we adopt the same superpotential, replace $f_{\mathcal{R}}$ above with $f_{\mathcal{R}} = c_+\phi^2$ and impose the IG and unification conditions. The last ones allow us to fully determine r_{\pm} achieving, thereby, more robust predictions than those presented in Ref. [20–23]. Most notably, the level of the predicted primordial gravitational waves is about an order of magnitude lower than the present upper bound [13, 33] and may be detectable in the next generation of experiments [34–37]. On the other hand, the IGHl can be constructed even

without the aforementioned kinetic mixing. This kind of models are briefly discussed in Appendix A and compared with the ones analyzed in the main text for completeness and clarity.

We exemplify our proposal employing as ‘‘GUT’’ gauge symmetry $G_{B-L} = G_{\text{SM}} \times U(1)_{B-L}$, where $G_{\text{SM}} = SU(3)_C \times SU(2)_L \times U(1)_Y$ is the gauge symmetry of the standard model, and B and L denote baryon and lepton number respectively – cf. Ref. [20, 22, 23, 27]. The embedding of IGHI within this particle model gives us the opportunity to connect inflation with low energy phenomenology. In fact, the absence of the gauge anomalies enforces the presence of three right-handed neutrinos N_i^c which, in turn, generate the tiny neutrino masses via the type I seesaw mechanism. Furthermore, the out-of-equilibrium decay of the N_i^c 's provides us with an explanation of the observed *baryon asymmetry of the universe* (BAU) [38] via *non-thermal leptogenesis* (nTL) [39] consistently with the gravitino (\tilde{G}) constraint [40–43] and the data [44, 45] on the neutrino oscillation parameters. Also, taking advantage of the adopted R symmetry, the parameter μ appearing in the mixing term between the two electroweak Higgs fields in the superpotential of MSSM is explained as in Refs. [3, 23, 25] via the v.e.v of the stabilizer field, provided that the relevant coupling constant is appropriately suppressed. The post-inflationary completion induces more constraints testing further the viability of our models.

The remaining text is organized into three sections. We first establish and analyze the inflationary scenario in Sec. II. We then – in Sec. III – examine a possible post-inflationary completion of our setting. Our conclusions are summarized in Sec. IV. Models of IGHI arising from alternative Kähler potentials are investigated in Appendix A. Throughout the text, the subscript of type $,z$ denotes derivation *with respect to* (w.r.t) the field z , and charge conjugation is denoted by a star. Unless otherwise stated, we use units where $m_{\text{P}} = 2.433 \cdot 10^{18}$ GeV is taken to be unity.

II. INFLATIONARY MODEL

In Sec. IIA we describe the generic formulation of IG models within SUGRA, in Sec. IIB, we construct the inflationary potential, and in Sec. IIC we analyze the observational consequences of the models.

A. EMBEDDING INDUCED-GRAVITY HI IN SUGRA

The implementation of IGHI requires the determination of the relevant super- and Kähler potentials, which are specified in Sec. IIA 1. In Sec. IIA 2 we present the form of the action in the two relevant frames and in Sec. IIA 3 we impose the IG constraint.

1. Set-up

As we already mentioned, we base the construction of our models on the superpotential

$$W_{\text{HI}} = \lambda S (\bar{\Phi}\Phi - M^2/4) \quad (1)$$

which is already introduced in the context of models of F-term hybrid inflation [24]. Here $\bar{\Phi}, \Phi$ denote a pair of left-handed chiral superfields oppositely charged under $U(1)_{B-L}$; S is a G_{B-L} -singlet chiral superfield; λ and M are parameters which can be made positive by field redefinitions. W_{HI} is the most general renormalizable superpotential consistent with a continuous R symmetry [24] under which

$$S \rightarrow e^{i\alpha} S, \bar{\Phi}\Phi \rightarrow \bar{\Phi}\Phi, W_{\text{HI}} \rightarrow e^{i\alpha} W_{\text{HI}}. \quad (2)$$

Here and in the subsequent discussion the subscript HI is frequently used instead of IGHI to simplify the notation.

As we verify below, W_{HI} allows us to break the gauge symmetry of the theory in a simple, elegant and restrictive way. The v.e.v.s of these fields, though, have to be related with the size of m_{P} according to the IG requirement. To achieve this, together with the establishment of an inflationary era, we have to combine W_{HI} with *one* of the following Kähler potentials which respect the (gauge and global) symmetries of W_{HI} and incorporate only quadratic terms of the various fields – cf. Ref. [23]:

$$K_1 = -N \ln(c_+ F_+ + F_{1S}(|S|^2)) + c_- F_-, \quad (3a)$$

$$K_2 = -N \ln(c_+ F_+) + c_- F_- + F_{2S}(|S|^2), \quad (3b)$$

$$K_3 = -N \ln(c_+ F_+) + F_{3S}(F_-, |S|^2), \quad (3c)$$

where $N > 0$. The functions $F_{\pm} = |\Phi \pm \bar{\Phi}^*|^2$ assist us in the introduction of a softly broken shift symmetry for the Higgs fields – cf. Ref. [20, 31]. In particular, the dominant shift symmetry adopted here is

$$\Phi \rightarrow \Phi + c \text{ and } \bar{\Phi} \rightarrow \bar{\Phi} + c^* \text{ with } c \in \mathbb{C}, \quad (4)$$

under which F_- remains unaltered. This has a string theoretical origin as shown in Ref. [47]. In this framework, mainly integer N 's are considered which can be reconciled with the observational data – see Sec. IIC 2. Namely, $N = 3$ [$N = 2$] for $K = K_1$ [$K = K_2$ or K_3] yields completely acceptable results. However, the deviation of the N 's from these integer values is also acceptable [5, 20, 22, 23, 48] and assist us to cover the whole allowed domain of the observables. In all K 's, F_+ expresses the violation of the symmetry in Eq. (4) and is placed in the argument of a logarithm with coefficient $(-N)$, whereas F_- is outside it. The crucial difference of the K 's considered here, compared to those employed in Ref. [23], is that unity does not accompany $c_+ F_+$. As explained in Sec. IIA 3, the identification of $c_+ F_+$ with unity at the vacuum of the theory essentially encapsulates the IG hypothesis – cf. Ref. [3, 5]. The degree of the violation of the symmetry in Eq. (4) is expressed by $r_{\pm} = c_+/c_-$, which is constrained by the unification condition to values of the order 0.1 – see Sec. IIB 3. Since this value is quite natural we are

not forced here to invoke any argument regarding its naturalness – cf. Ref. [23].

The functions F_{lS} with $l = 1, 2, 3$ encountered in Eqs. (3a) – (3c) support canonical normalization and safe stabilization of S during and after IGHI. Their possible forms are given in Ref. [23]. Just for definiteness, we adopt here only their logarithmic form, i.e.,

$$F_{1S} = -\ln(1 + |S|^2/N), \quad (5a)$$

$$F_{2S} = N_S \ln(1 + |S|^2/N_S), \quad (5b)$$

$$F_{3S} = N_S \ln(1 + |S|^2/N_S + c_- F_-/N_S), \quad (5c)$$

with $0 < N_S < 6$. Recall [6, 46] that the simplest term $|S|^2$ leads to instabilities for $K = K_1$ and light excitations for $K = K_2$ and K_3 . The heaviness of these modes is required so that the observed curvature perturbation is generated wholly by our inflaton in accordance with the lack of any observational hint [53] for large non-Gaussianity in the cosmic microwave background.

2. From Einstein to Jordan Frame

With the ingredients above we can extract the part of the *Einstein frame* (EF) action within SUGRA related to the complex scalars $z^\alpha = S, \Phi, \bar{\Phi}$ – denoted by the same superfield symbol. This has the form [46]

$$S = \int d^4x \sqrt{-\hat{g}} \left(-\frac{1}{2} \hat{\mathcal{R}} + K_{\alpha\bar{\beta}} \hat{g}^{\mu\nu} D_\mu z^\alpha D_\nu z^{*\bar{\beta}} - \hat{V} \right), \quad (6a)$$

where $\hat{\mathcal{R}}$ is the EF Ricci scalar curvature, D_μ is the gauge covariant derivative, $K_{\alpha\bar{\beta}} = K_{,z^\alpha z^{*\bar{\beta}}}$, and $K^{\alpha\bar{\beta}} K_{\bar{\beta}\gamma} = \delta_\gamma^\alpha$. Also, \hat{V} is the EF SUGRA potential which can be found in terms of W_{HI} in Eq. (1) and the K 's in Eqs. (3a) – (3c) via the formula

$$\hat{V} = e^K \left(K^{\alpha\bar{\beta}} (D_\alpha W_{\text{HI}}) D_{\bar{\beta}}^* W_{\text{HI}}^* - 3|W_{\text{HI}}|^2 \right) + \frac{g^2}{2} \sum_a D_a^2, \quad (6b)$$

where $D_\alpha W_{\text{HI}} = W_{\text{HI},z^\alpha} + K_{,z^\alpha} W_{\text{HI}}$, $D_a = z^\alpha (T_a)_\alpha^\beta K_\beta$ and the summation is applied over the generators T_a of G_{B-L} . In the *right-hand side* (r.h.s) of the equation above we clearly recognize the contribution from the D terms (proportional to g^2) and the remaining one which comes from the F terms.

If we perform a conformal transformation, along the lines of Ref. [20, 46], defining the frame function as

$$-\Omega/N = \exp(-K/N) \Rightarrow K = -N \ln(-\Omega/N), \quad (7)$$

we can obtain the form of S in the *Jordan Frame* (JF) which is written as [20]

$$S = \int d^4x \sqrt{-g} \left(\frac{\Omega}{2N} \mathcal{R} - \frac{27}{N^3} \Omega \mathcal{A}_\mu \mathcal{A}^\mu - V + \left(\Omega_{\alpha\bar{\beta}} + \frac{3-N}{N} \frac{\Omega_\alpha \Omega_{\bar{\beta}}}{\Omega} \right) D_\mu z^\alpha D^\mu z^{*\bar{\beta}} \right), \quad (8a)$$

where we use the shorthand notation $\Omega_\alpha = \Omega_{,z^\alpha}$, and $\Omega_{\bar{\alpha}} = \Omega_{,z^{*\bar{\alpha}}}$. We also set $V = \hat{V} \Omega^2/N^2$ and

$$\mathcal{A}_\mu = -iN (\Omega_\alpha D_\mu z^\alpha - \Omega_{\bar{\alpha}} D_\mu z^{*\bar{\alpha}}) / 6\Omega. \quad (8b)$$

It is easy to verify that the expression in the parenthesis of the second line in Eq. (8a), for the K 's considered in Sec. II A 1, is not only different than $\delta_{\alpha\bar{\beta}}$ but also includes entries proportional to and dominated by $c_- \gg c_+$. For this reason the IGHI analyzed below may be more properly characterized as kinetically modified. Most importantly, though, the first term in the first line of the r.h.s of Eq. (8a) reveals that $-\Omega/N$ plays the role of a non-minimal coupling to gravity. Comparing Eq. (7) with the K 's in Eqs. (3a) – (3c) we can infer that

$$-\Omega/N = c_+ F_+, \quad (9)$$

along the field configuration

$$\Phi = \bar{\Phi}^* \quad \text{and} \quad S = 0, \quad (10)$$

which is a honest inflationary trajectory, as shown in Sec. II B 2. The identification of the quantity in Eq. (9) with m_{P}^2 at the vacuum, according to the IG conjecture, can be accommodated as described in the next section.

3. Induced-Gravity Requirement

The implementation of the IG scenario requires the generation of m_{P} at the vacuum of the theory, which thereby has to be determined. To do this we have to compute V in Eq. (6b) for small values of the various fields, expanding it in powers of $1/m_{\text{P}}$. Namely, we obtain the following low-energy effective potential

$$V_{\text{eff}} = e^{\tilde{K}} \tilde{K}^{\alpha\bar{\beta}} W_{\text{HI}\alpha} W_{\text{HI}\bar{\beta}}^* + \frac{g^2}{2} \sum_a D_a^2 + \dots, \quad (11a)$$

where the ellipsis represents terms proportional to W_{HI} or $|W_{\text{HI}}|^2$ which obviously vanish along the path in Eq. (49) – we assume here that the vacuum is contained in the inflationary trajectory. Also, \tilde{K} is the limit of the K 's in Eqs. (3a) – (3c) for $m_{\text{P}} \rightarrow \infty$. The absence of unity in the arguments of the logarithms multiplied by N in Eqs. (3a) – (3c) prevents the drastic simplification of \tilde{K} , especially for $K = K_1$ – cf. Ref. [23]. As a consequence, the expression of the resulting V_{eff} is rather lengthy. For this reason we confine ourselves below to $K = K_2$ or K_3 where F_{lS} with $l = 2, 3$ is placed outside the first logarithm and so \tilde{K} can be significantly simplified. Namely, we get

$$\tilde{K} = -N \ln c_+ F_+ + c_- F_- + |S|^2, \quad (11b)$$

from which we can then compute

$$\left(\tilde{K}_{\alpha\bar{\beta}} \right) = \text{diag} \left(\tilde{M}_\pm, 1 \right) \quad \text{with} \quad \tilde{M}_\pm = \begin{pmatrix} c_- & \tilde{K}_{\Phi\bar{\Phi}^*} \\ \tilde{K}_{\Phi\bar{\Phi}^*} & c_- \end{pmatrix}. \quad (12a)$$

Here,

$$\tilde{K}_{\Phi\bar{\Phi}^*} = \frac{N}{(\Phi + \bar{\Phi}^*)^2} \quad \text{and} \quad \tilde{K}_{\bar{\Phi}\Phi^*} = \frac{N}{(\Phi^* + \bar{\Phi})^2}, \quad (12b)$$

since

$$\tilde{K}_{\Phi} = -N/(\Phi + \bar{\Phi}^*) + c_-(\Phi^* - \bar{\Phi}) \quad (12c)$$

and

$$\tilde{K}_{\bar{\Phi}} = -N/(\Phi^* + \bar{\Phi}) - c_-(\Phi - \bar{\Phi}^*). \quad (12d)$$

To compute V_{eff} we need to know

$$\left(\tilde{K}^{\alpha\bar{\beta}}\right) = \text{diag}\left(\tilde{M}_{\pm}^{-1}, 1\right), \quad (13a)$$

where

$$\tilde{M}_{\pm}^{-1} = \frac{1}{\det\tilde{M}_{\pm}} \begin{pmatrix} c_- & -\tilde{K}_{\Phi\bar{\Phi}^*} \\ -\tilde{K}_{\bar{\Phi}\Phi^*} & c_- \end{pmatrix}, \quad (13b)$$

with

$$\det\tilde{M}_{\pm} = c_-^2 - N^2/F_+^2. \quad (13c)$$

Upon substitution of Eqs. (13a) and (13b) into Eq. (11a) we obtain

$$V_{\text{eff}} \simeq \lambda^2 e^{\tilde{K}_+} \left| \bar{\Phi}\Phi - \frac{1}{4}M^2 \right|^2 + \frac{g^2}{2} \left(\Phi\tilde{K}_{\Phi} - \bar{\Phi}\tilde{K}_{\bar{\Phi}} \right)^2 + \frac{\lambda^2 e^{\tilde{K}_+} |S|^2}{\det\tilde{M}_{\pm}} \left(c_- (|\Phi|^2 + |\bar{\Phi}|^2) - \tilde{K}_{\Phi\bar{\Phi}^*} \bar{\Phi}\Phi^* - \tilde{K}_{\bar{\Phi}\Phi^*} \Phi^*\bar{\Phi} \right), \quad (14)$$

where $\tilde{K}_+ = -N \ln c_+ F_+$. We remark that the direction in Eq. (49) assures D-flatness since $\langle \Phi\tilde{K}_{\Phi} \rangle = \langle \bar{\Phi}\tilde{K}_{\bar{\Phi}} \rangle$ and so the vacuum lies along it with

$$\langle S \rangle = 0 \quad \text{and} \quad |\langle \Phi \rangle| = |\langle \bar{\Phi} \rangle| = M/2. \quad (15)$$

The same result holds also for $K = K_1$ as we can verify after a more tedious computation. Eq. (15) means that $\langle \Phi \rangle$ and $\langle \bar{\Phi} \rangle$ spontaneously break $U(1)_{B-L}$ down to \mathbb{Z}_2^{B-L} . Note that $U(1)_{B-L}$ is already broken during IGH1 and so no cosmic string are formed – contrary to what happens in the models of the standard F-term hybrid inflation [25, 26], which also employ W_{HI} in Eq. (1).

Inserting Eq. (15) into Eq. (9) we deduce that the conventional Einstein gravity can be recovered at the vacuum if

$$c_+ \langle F_+ \rangle = 1 \quad \Rightarrow \quad M = 1/\sqrt{c_+}. \quad (16)$$

For $c_+ \sim (10^2 - 10^3)$ employed here, the resulting values of M are theoretically quite natural since they lie close to unity. Indeed, since the form of W_{HI} in Eq. (1) is established around m_{P} we expect that the scales entered by hand in the theory have comparable size.

B. INFLATIONARY POTENTIAL

Below we outline the derivation of the inflationary potential in Sec. II B 1 and check its stability by computing one-loop corrections in Sec. II B 2. The last part of the analysis allows us to determine the gauge-coupling unification condition (see Sec. II B 3) which assists us to further constrain our model.

1. Tree-Level Result

If we express Φ , $\bar{\Phi}$ and S according to the parametrization

$$\Phi = \frac{\phi e^{i\theta}}{\sqrt{2}} \cos \theta_{\Phi}, \quad \bar{\Phi} = \frac{\phi e^{i\bar{\theta}}}{\sqrt{2}} \sin \theta_{\Phi} \quad \text{and} \quad S = \frac{s + i\bar{s}}{\sqrt{2}}, \quad (17)$$

with $0 \leq \theta_{\Phi} \leq \pi/2$, the trough in Eq. (49) can be written as

$$\bar{s} = s = \theta = \bar{\theta} = 0 \quad \text{and} \quad \theta_{\Phi} = \pi/4. \quad (18)$$

Along this the only surviving term in Eq. (6b) is

$$\widehat{V}_{\text{HI}} = e^K K^{SS^*} |W_{\text{HI},S}|^2, \quad (19a)$$

which, for the choices of K 's in Eqs. (3a) – (3c), reads

$$\widehat{V}_{\text{HI}} = \frac{\lambda^2 f_{\text{W}}^2}{16c_+^2} f_{\mathcal{R}}^{-N} \cdot \begin{cases} f_{\mathcal{R}} & \text{for } K = K_1, \\ 1 & \text{for } K = K_2 \text{ and } K_3, \end{cases} \quad (19b)$$

where we define the (inflationary) frame function as

$$f_{\mathcal{R}} = -\frac{\Omega}{N} \Big|_{\text{Eq. (18)}} = c_+ \phi^2. \quad (19c)$$

The last factor in Eq. (19b) originates from the expression of K^{SS^*} for the various K 's. Also $f_{\text{W}} = c_+ \phi^2 - 1$ arises from the last factor in the r.h.s of Eq. (19a) and $f_{\mathcal{R}}^{-N} = e^K$. If we set

$$N = \begin{cases} 2n + 3 & \text{for } K = K_1, \\ 2(n + 1) & \text{for } K = K_2 \text{ and } K_3, \end{cases} \quad (19d)$$

we arrive at a universal expression for \widehat{V}_{HI} which is

$$\widehat{V}_{\text{HI}} = \frac{\lambda^2 f_{\text{W}}^2}{16c_+^2 f_{\mathcal{R}}^{2(1+n)}}. \quad (20)$$

The value $n = 0$ is special since we get $N = 3$ for $K = K_1$ and $N = 2$ for $K = K_2$ or K_3 . Therefore, \widehat{V}_{HI} develops an inflationary plateau as in the original case of Starobinsky model within no-scale SUGRA [3, 6]. Contrary to that case, though, here we also have c_- , which dominates the canonical normalization of ϕ , and n , whose variation may have an important impact on the observables – cf. Ref. [20, 22]. In particular, for $n < 0$, \widehat{V}_{HI} remains an increasing function of ϕ , whereas for $n > 0$, it develops a local maximum

$$\widehat{V}_{\text{HI}}(\phi_{\text{max}}) = \frac{\lambda^2 n^{2n}}{16c_+^2 (1+n)^{2(1+n)}} \quad \text{at} \quad \phi_{\text{max}} = \sqrt{\frac{1+n}{c_+ n}}. \quad (21)$$

TABLE I: Mass-squared spectrum of the inflaton sector for $K = K_1, K_2$ and K_3 along the path in Eq. (18).

FIELDS	EIGENSTATES	MASSES SQUARED			
			$K = K_1$	$K = K_2$	$K = K_3$
4 Real Scalars	$\hat{\theta}_+$	$\hat{m}_{\theta_+}^2$	$6\hat{H}_{\text{HI}}^2$		$6(1 + 1/N_S)\hat{H}_{\text{HI}}^2$
	$\hat{\theta}_\Phi$	$\hat{m}_{\theta_\Phi}^2$	$M_{BL}^2 + 6\hat{H}_{\text{HI}}^2$		$M_{BL}^2 + 6(1 + 1/N_S)\hat{H}_{\text{HI}}^2$
	$\hat{s}, \hat{\bar{s}}$	\hat{m}_s^2	$6f_W\hat{H}_{\text{HI}}^2/N$	$6\hat{H}_{\text{HI}}^2/N_S$	
1 Gauge Boson	A_{BL}	M_{BL}^2	$g^2(c_- \phi^2 - N)$		
4 Weyl Spinors	$\hat{\psi}_\pm = (\hat{\psi}_\Phi \pm \hat{\psi}_S)/\sqrt{2}$	$\hat{m}_{\psi_\pm}^2$	$6(N - c_+(N - 2)\phi^2)^2 \hat{H}_{\text{HI}}^2 / c_- f_W^2 \phi^2$		
	$\lambda_{BL}, \hat{\psi}_{\Phi-}$	M_{BL}^2	$g^2(c_- \phi^2 - N)$		

In a such case we are forced to assume that hilltop [49] IGHI occurs with ϕ rolling from the region of the maximum down to smaller values. The relevant tuning of the initial conditions can be quantified by defining [26] the quantity

$$\Delta_{\text{max}\star} = (\phi_{\text{max}} - \phi_\star) / \phi_{\text{max}}, \quad (22)$$

where ϕ_\star is the value of ϕ when the pivot scale $k_\star = 0.05/\text{Mpc}$ crosses outside the inflationary horizon. The naturalness of the attainment of IGHI increases with $\Delta_{\text{max}\star}$, and it is maximized when $\phi_{\text{max}} \gg \phi_\star$ which results in $\Delta_{\text{max}\star} \simeq 1$.

To specify the EF canonically normalized inflaton, we note that, for all choices of K in Eqs. (3a) – (3c), $K_{\alpha\beta}$ along the configuration in Eq. (18) takes the form

$$(K_{\alpha\beta}) = \text{diag}(M_\pm, K_{SS^\star}) \quad \text{with} \quad M_\pm = \begin{pmatrix} c_- & N/\phi^2 \\ N/\phi^2 & c_- \end{pmatrix}, \quad (23)$$

where $K_{SS^\star} = 1/f_{\mathcal{R}} [K_{SS^\star} = 1]$ for $K = K_1 [K = K_2$ and $K_3]$. Upon diagonalization of M_\pm we find its eigenvalues which are

$$\kappa_\pm = c_- \pm N/\phi^2. \quad (24)$$

Given that the lowest ϕ value is $\langle \phi \rangle = 1/\sqrt{c_+}$, we can impose a robust restriction on the parameters to assure the positivity of κ_- during and after IGHI. Namely,

$$\kappa_- \gtrsim 0 \Rightarrow r_\pm \lesssim 1/N. \quad (25)$$

Inserting Eqs. (17) and (23) in the second term of the r.h.s of Eq. (6a) we can define the EF canonically normalized fields, denoted by hat, as follows

$$\frac{d\hat{\phi}}{d\phi} = J = \sqrt{\kappa_+}, \quad \hat{\theta}_+ = \frac{J\phi\theta_+}{\sqrt{2}}, \quad \hat{\theta}_- = \sqrt{\frac{\kappa_-}{2}}\phi\theta_-, \quad (26a)$$

$$\hat{\theta}_\Phi = \phi\sqrt{\kappa_-}(\theta_\Phi - \pi/4), \quad (\hat{s}, \hat{\bar{s}}) = \sqrt{K_{SS^\star}}(s, \bar{s}), \quad (26b)$$

where $\theta_\pm = (\bar{\theta} \pm \theta)/\sqrt{2}$. Note, in passing, that the spinors ψ_S and $\psi_{\Phi\pm}$ associated with the superfields S and $\Phi - \bar{\Phi}$ are similarly normalized, i.e., $\hat{\psi}_S = \sqrt{K_{SS^\star}}\psi_S$ and $\hat{\psi}_{\Phi\pm} = \sqrt{\kappa_\pm}\psi_{\Phi\pm}$ with $\psi_{\Phi\pm} = (\psi_\Phi \pm \psi_{\bar{\Phi}})/\sqrt{2}$.

2. Stability and Loop-Corrections

We can verify that the inflationary direction in Eq. (18) is stable w.r.t the fluctuations of the non-inflaton fields. To this end, we construct the mass-squared spectrum of the various scalars defined in Eqs. (26a) and (26b). Taking the limit $c_- \gg c_+$ we find the expressions of the masses squared $\hat{m}_{\chi^\alpha}^2$ (with $\chi^\alpha = \theta_+, \theta_\Phi$ and S) arranged in Table I. For $\phi \simeq \phi_\star$ these fairly approach the quite lengthy, exact expressions taken into account in our numerical computation. We infer that \hat{m}_s^2 stays positive for $K = K_1$ and $0 < N < 6$ and heavy enough, i.e. $\hat{m}_{z^\alpha}^2 \gg \hat{H}_{\text{HI}}^2 = \hat{V}_{\text{HI}}/3$, for $K = K_2$ and K_3 for $0 < N_S < 6$. In Table I we also display the masses, M_{BL} , of the gauge boson A_{BL} – which signals the fact that G_{B-L} is broken during IGHI – and the masses of the corresponding fermions. As a consequence, let us again emphasize that no cosmic string are produced at the end of IGHI.

The derived mass spectrum can be employed in order to find the one-loop radiative corrections, $\Delta\hat{V}_{\text{HI}}$, to \hat{V}_{HI} . Considering SUGRA as an effective theory with cutoff scale equal to m_P , the well-known Coleman-Weinberg formula [50] can be employed taking into account only the masses which lie well below m_P , i.e., all the masses arranged in Table I besides M_{BL} and \hat{m}_{θ_Φ} . The resulting $\Delta\hat{V}_{\text{HI}}$ leaves intact our inflationary outputs, provided that the renormalization-group mass scale Λ , is determined by requiring $\Delta\hat{V}_{\text{HI}}(\phi_\star) = 0$ or $\Delta\hat{V}_{\text{HI}}(\phi_f) = 0$. These conditions yield $\Lambda \simeq 3.2 \cdot 10^{-5} - 1.4 \cdot 10^{-4}$ and render our results practically independent of Λ since these can be derived exclusively by using \hat{V}_{HI} in Eq. (20) with the various quantities evaluated at Λ – cf. Ref. [20]. Note that their renormalization-group running is expected to be negligible because Λ is close to the inflationary scale $\hat{V}_{\text{HI}}^{1/4} \simeq (3 - 7) \cdot 10^{-3}$.

3. SUSY Gauge Coupling Unification

The mass M_{BL} listed in Table I of the gauge boson A_{BL} may, in principle, be a free parameter since the $U(1)_{B-L}$ gauge symmetry does not disturb the unification of the MSSM gauge coupling constants. To be more specific, though, we prefer to determine M_{BL} by requiring that it takes the value

$M_{\text{GUT}} \simeq 2/2.43 \cdot 10^{-2} = 8.22 \cdot 10^{-3}$ dictated by this unification. Namely, we impose

$$\langle M_{BL} \rangle = M_{\text{GUT}}. \quad (27)$$

The condition above allows us to fix r_{\pm} , since substituting Eq. (16) in M_{BL} shown in Table I, we obtain

$$g^2 (c_- \langle \phi \rangle^2 - N) = M_{\text{GUT}}^2 \Rightarrow r_{\pm} = \frac{g^2}{Ng^2 + M_{\text{GUT}}^2}, \quad (28)$$

with $g \simeq 0.7$ being the value of the unified coupling constant within MSSM. Since $M_{\text{GUT}} > 0$ the condition above satisfies the restriction in Eq. (25) yielding r_{\pm} close to its upper bound because $M_{\text{GUT}} \ll 1$. As a consequence, r_{\pm} ceases to be a free parameter, in sharp contrast to the models of Ref. [21, 23] where Eq. (27) is employed to extract $M \ll 1$ as a function of n and r_{\pm} without any other theoretical constraint between them. Here the interplay of Eqs. (16) and (28) leads to the reduction of the free parameters by one, thereby rendering the present set-up more restrictive and predictive.

C. INFLATION ANALYSIS

In Sec. II C 2 below we inspect if the potential in Eq. (20) endowed with the condition of Eqs. (16) and (28) may be consistent with a number of observables introduced in Sec. II C 1. Given that the analysis of inflation in both EF and JF yields equivalent results [9], we carry it out exclusively in the EF. A crucial difference of the present analysis w.r.t that for the models in Ref. [20–23] is that M , given by Eq. (16), is not negligible during the inflationary period and enters the relevant formulas via the function f_W defined below Eq. (19b).

1. Inflationary Observables

The period of slow-roll IGHI is determined in the EF by the condition

$$\max\{\hat{\epsilon}(\phi), |\hat{\eta}(\phi)|\} \leq 1, \quad (29a)$$

where the slow-roll parameters [51],

$$\hat{\epsilon} = \left(\frac{\widehat{V}_{\text{HI}, \widehat{\phi}}}{\sqrt{2\widehat{V}_{\text{HI}}}} \right)^2 \quad \text{and} \quad \hat{\eta} = \frac{\widehat{V}_{\text{HI}, \widehat{\phi\phi}}}{\widehat{V}_{\text{HI}}}, \quad (29b)$$

can be derived employing J in Eq. (20), without explicitly expressing \widehat{V}_{HI} in terms of $\widehat{\phi}$. Our results are

$$\hat{\epsilon} = \frac{8(1+n - nc_+ \phi^2)^2}{c_- \phi^2 f_W^2}; \quad (30a)$$

$$\frac{\hat{\eta}}{4} = \frac{5 + 9n - (3 + 10n)c_+ \phi^2 + 4n^2 f_W^2 + nc_+^2 \phi^2}{c_- \phi^2 f_W^2}. \quad (30b)$$

Given that $\phi \ll 1$, Eq. (29a) is saturated at the maximal ϕ value, ϕ_f , from the following two values

$$\phi_{1f} \simeq \sqrt{\frac{2}{c_-}} \frac{1}{r_{\pm}^{1/3}} \quad \text{and} \quad \phi_{2f} \simeq \sqrt{\frac{2}{c_-}} \left(\frac{3}{r_{\pm}} \right)^{1/4}, \quad (31)$$

where ϕ_{1f} and ϕ_{2f} are such that $\hat{\epsilon}(\phi_{1f}) \simeq 1$ and $\hat{\eta}(\phi_{2f}) \simeq 1$. The n dependence is not so crucial for this estimation.

The number of e-foldings \widehat{N}_{\star} that the scale $k_{\star} = 0.05/\text{Mpc}$ experiences during IGHI and the amplitude A_s of the power spectrum of the curvature perturbations generated by ϕ can be computed using the standard formulae [51]

$$\widehat{N}_{\star} = \int_{\widehat{\phi}_f}^{\widehat{\phi}_{\star}} d\widehat{\phi} \frac{\widehat{V}_{\text{HI}}}{\widehat{V}_{\text{HI}, \widehat{\phi}}} \quad \text{and} \quad A_s^{1/2} = \frac{1}{2\sqrt{3}\pi} \frac{\widehat{V}_{\text{HI}}^{3/2}(\widehat{\phi}_{\star})}{|\widehat{V}_{\text{HI}, \widehat{\phi}}(\widehat{\phi}_{\star})|}, \quad (32)$$

where $\widehat{\phi}_{\star}$ [$\widehat{\phi}_{\star}$] is the value of ϕ [$\widehat{\phi}$] when k_{\star} crosses the inflationary horizon. Since $\phi_{\star} \gg \phi_f$, from Eq. (32) we find

$$\widehat{N}_{\star} \simeq \begin{cases} c_- \phi_{\star}^2 (c_- r_{\pm} \phi_{\star}^2 / 2 - 1) / 8 & \text{for } n = 0, \\ - \left(nc_+ \phi_{\star}^2 + \ln \left(1 - \frac{nc_+ \phi_{\star}^2}{1+n} \right) \right) / 8n^2 r_{\pm} & \text{for } n \neq 0, \end{cases} \quad (33)$$

where $\widehat{\phi}_{\star}$ is the value of $\widehat{\phi}$ when k_{\star} crosses the inflationary horizon. Note that $nr_{\pm} \widehat{\phi}_{\star}^2 < 1$ for all relevant cases. Solving the equations above w.r.t ϕ_{\star} , we can express ϕ_{\star} in terms of \widehat{N}_{\star} as follows

$$\phi_{\star} \simeq \frac{f_{\mathcal{R}\star}^{1/2}}{c_+^{1/2}} \quad \text{with} \quad f_{\mathcal{R}\star} = \begin{cases} 1 + \left(1 + 16r_{\pm} \widehat{N}_{\star} \right)^{1/2} & \text{for } n = 0, \\ (1 + n + W_k(y)) / n & \text{for } n \neq 0, \end{cases} \quad (34)$$

where we make use of Eq. (19c). Also, W_k is the Lambert W (or product logarithmic) function [52] with

$$y = -(1+n) \exp \left(-1 - n(1 + 8n \widehat{N}_{\star} r_{\pm}) \right). \quad (35)$$

We take $k = 0$ for $n > 0$ and $k = -1$ for $n < 0$.

For any n we can impose a lower bound on c_- , above which $\phi_{\star} \leq 1$. Indeed, from Eq. (34) we have

$$\phi_{\star} \leq 1 \Rightarrow c_- \geq f_{\mathcal{R}\star} / r_{\pm}, \quad (36)$$

and so our proposal can be stabilized against corrections from higher order terms of the form $(\Phi \bar{\Phi})^p$ with $p > 1$ in W_{HI} – see Eq. (1). Despite the fact that c_- may take relatively large values, the corresponding effective theories are valid [14, 15] up to $m_{\text{P}} = 1$ for r_{\pm} given by Eq. (28). To further clarify this point we have to identify the ultraviolet cut-off scale Λ_{UV} of the theory by analyzing the small-field behavior of our models. More specifically, we expand about $\langle \phi \rangle = M$ – see Eq. (16) – the second term in the r.h.s of Eq. (6a) for $\mu = \nu = 0$ and \widehat{V}_{HI} in Eq. (20). Our results can be written in terms of $\widehat{\phi}$ as follows

$$J^2 \dot{\phi}^2 \simeq \left(1 + Nr_{\pm} - 2r_{\pm} \bar{r}_{\pm} \widehat{\delta\phi} + 3N \bar{r}_{\pm}^2 \widehat{\delta\phi}^2 + \dots \right) \widehat{\delta\phi}^2, \quad (37a)$$

where we set $\bar{r}_{\pm} = \sqrt{r_{\pm}/(1 + Nr_{\pm})}$, and

$$\widehat{V}_{\text{HI}} \simeq \frac{\lambda^2 \bar{r}_{\pm}^2 \widehat{\delta\phi}^2}{4c_+^2} \left(1 - (3 + 4n) \bar{r}_{\pm} \widehat{\delta\phi} + \left(\frac{25}{4} + 14n + 8n^2 \right) \bar{r}_{\pm}^2 \widehat{\delta\phi}^2 + \dots \right). \quad (37b)$$

From the expressions above we conclude that $\Lambda_{UV} = m_P$ since $r_{\pm} \leq 1$ (and so $\bar{r}_{\pm} \leq 1$) due to Eq. (28). Although these expansions are valid only during reheating we consider the Λ_{UV} extracted this way as the overall cut-off scale of the theory since reheating is regarded [15] as an unavoidable stage of IGHI.

From the second equation in Eq. (32) we can also conclude that λ is proportional to c_- for fixed n . Indeed, plugging Eq. (34) into this equation and solving w.r.t λ , we find

$$\lambda = 32\sqrt{3A_s}\pi c_- r_{\pm}^{3/2} f_{\mathcal{R}\star}^{n+1/2} \frac{n(1-f_{\mathcal{R}\star})+1}{(f_{\mathcal{R}\star}-1)^2}. \quad (38)$$

Numerically, – see below – we find that λ/c_- develops a maximum at $n \simeq -0.15$ which signals a transition to a branch of inflationary solutions which deviate from those obtained within the Starobinsky-like inflation.

The (scalar) spectral index n_s , its running a_s , and the scalar-to-tensor ratio r are found from the relations [51]

$$n_s = 1 - 6\hat{\epsilon}_{\star} + 2\hat{\eta}_{\star}, \quad r = 16\hat{\epsilon}_{\star}, \quad (39a)$$

$$a_s = 2(4\hat{\eta}_{\star}^2 - (n_s - 1)^2)/3 - 2\hat{\xi}_{\star}, \quad (39b)$$

where the variables with subscript \star are evaluated at $\phi = \phi_{\star}$ and $\hat{\xi} = \hat{V}_{\text{HI},\phi} \hat{V}_{\text{HI},\phi\phi} / \hat{V}_{\text{HI}}^2$. Inserting $f_{\mathcal{R}\star}$ from Eq. (34) into Eqs. (39a) and (39b) we obtain

$$n_s \simeq 1 - \frac{8}{f_{\mathcal{R}\star}} \left(\frac{3f_{\mathcal{R}\star} + 1}{(f_{\mathcal{R}\star} - 1)^2} - n \frac{f_{\mathcal{R}\star} + 3}{f_{\mathcal{R}\star} - 1} + 2n^2 \right) \quad (40a)$$

$$r \simeq 128 \frac{r_{\pm}}{f_{\mathcal{R}\star}} \left(\frac{1 - n(f_{\mathcal{R}\star} - 1)}{f_{\mathcal{R}\star} - 1} \right)^2, \quad (40b)$$

$$\begin{aligned} a_s &\simeq \frac{64r_{\pm}^2}{3(f_{\mathcal{R}\star} - 1)^4 f_{\mathcal{R}\star}^2} (3 - 9f_{\mathcal{R}\star}(2f_{\mathcal{R}\star} + 1) \\ &+ 3(f_{\mathcal{R}\star} - 1)(f_{\mathcal{R}\star}(7f_{\mathcal{R}\star} + 9) - 4)n \\ &+ 2(f_{\mathcal{R}\star} - 1)^2(f_{\mathcal{R}\star}(f_{\mathcal{R}\star} - 42) + 121)n^2). \end{aligned} \quad (40c)$$

For $|n| < 0.1$ these formulas may be expanded successively in series of n and $1/\hat{N}_{\star}$ with results

$$n_s \simeq 1 - \frac{16}{3}n^2 r_{\pm} - 2n \frac{r_{\pm}^{1/2}}{\hat{N}_{\star}^{1/2}} - \frac{3 - 2n}{2\hat{N}_{\star}} - \frac{3 + 5n}{24(\hat{N}_{\star}^3 r_{\pm})^{1/2}}, \quad (41a)$$

$$r \simeq -\frac{8n}{\hat{N}_{\star}} - \frac{1}{2\hat{N}_{\star}^2 r_{\pm}} + \frac{2(3 + 2n)}{3(\hat{N}_{\star}^3 r_{\pm})^{1/2}} + \frac{32n^2 r_{\pm}^{1/2}}{3\hat{N}_{\star}^{1/2}}, \quad (41b)$$

$$a_s \simeq -\frac{nr_{\pm}^{1/2}}{\hat{N}_{\star}^{3/2}} - \frac{3 - 2n}{2\hat{N}_{\star}^2}. \quad (41c)$$

From the expressions above, we can infer that there is a clear n (and r_{\pm}) dependence of the observables which deviate somewhat from those obtained in the pure Starobinsky-type inflation (or IG inflation) [3, 5, 6]. Note that the formulae, although similar, are not identical with those found in Ref. [23].

2. Comparison with Observations

The approximate analytic expressions above can be verified by the numerical analysis. Namely, we apply the accurate expressions in Eq. (32) and confront the corresponding observables with the requirements [53]

$$\hat{N}_{\star} \simeq 61.5 + \ln \frac{\hat{V}_{\text{HI}}(\phi_{\star})^{1/2}}{\hat{V}_{\text{HI}}(\phi_f)^{1/4}} + \frac{1}{2}f_{\mathcal{R}}(\phi_{\star}); \quad (42a)$$

$$A_s^{1/2} \simeq 4.627 \cdot 10^{-5}, \quad (42b)$$

adjusting ϕ_{\star} and λ/c_- . Note that in Eq. (42a) we consider an equation-of-state parameter $w_{\text{int}} = 1/3$ corresponding to quartic potential which is expected to approximate \hat{V}_{HI} rather well for $\phi \ll 1$ – see Ref. [20]. We obtain $\hat{N}_{\star} \simeq (57.5 - 60)$. Then, we compute the model predictions via Eqs. (39a) and (39b) for any selected n . The resulting values of n_s and r must be in agreement with the fitting of the data [13, 33] with $\Lambda\text{CDM}+r$ model. We take into account the data from *Planck* and *Baryon Acoustic Oscillations* (BAO) and the BK14 data taken by the BICEP2/Keck Array CMB polarization experiments up to and including the 2014 observing season. The results are

$$(a) \ n_s = 0.968 \pm 0.009 \quad \text{and} \quad (b) \ r \leq 0.07, \quad (43)$$

at 95% confidence level (c.l.) with $|a_s| \ll 0.01$.

Let us clarify here that the (theoretically) free parameters of our models are n and λ/c_- and not n , c_- , and λ as naively expected – recall that M and r_{\pm} are found from Eqs. (16) and (28). Indeed, if we perform the rescalings

$$\Phi \rightarrow \Phi/\sqrt{c_-}, \quad \bar{\Phi} \rightarrow \bar{\Phi}/\sqrt{c_-} \quad \text{and} \quad S \rightarrow S, \quad (44)$$

W in Eq. (1) depends on λ/c_- and r_{\pm}^{-1} , while the K 's in Eq. (3a) – (3c) depend on n and r_{\pm} . As a consequence, \hat{V}_{HI} depends exclusively on λ/c_- and n . Since the λ/c_- variation is rather trivial – see Eq. (38) – we focus below on the variation of n .

Our results are displayed in Fig. 1, where we show a comparison of the models' predictions against the observational data [13, 33] in the $n_s - r_{0.002}$ plane, where $r_{0.002} = 16\hat{\epsilon}(\hat{\phi}_{0.002})$ with $\hat{\phi}_{0.002}$ being the value of $\hat{\phi}$ when the scale $k = 0.002/\text{Mpc}$, which undergoes $\hat{N}_{0.002} = \hat{N}_{\star} + 3.22$ e-foldings during IGHI, crosses the horizon of IGHI. We depict the theoretically allowed values with solid and dashed lines for $K = K_2$ or K_3 and $K = K_1$ respectively. The variation of n is shown along each line. In squared brackets we display the n values for $K = K_1$ when these differ appreciably from those for $K = K_2$ or K_3 . We remark that for $n > 0$ there is a discrepancy of about 20% changing K from K_1 to K_2 or K_3 , which decreases as n decreases below zero. This effect originates from the difference in J – see Eqs. (24) and (26a) – which becomes smaller and smaller as n decreases or c_- increases. We observe that $n > 0$ values dominate the part of the curves with lower r values and $n_s \leq 0.973$, whereas the $n < 0$ values generate the part of the curves with n_s close

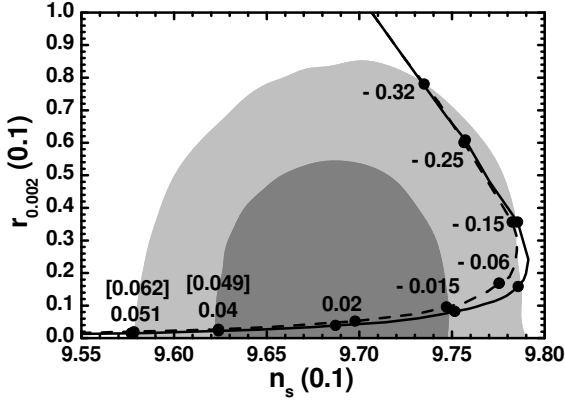


FIG. 1: Allowed curves in the $n_s - r_{0.002}$ plane for $K = K_1$ (dashed line) and $K = K_2$ or K_3 (solid line) with the n values indicated on the curves (the n values in squared brackets correspond to $K = K_1$). The marginalized joint 68% [95%] regions from Planck, BAO and BK14 data are depicted by the dark [light] shaded contours.

TABLE II: Parameters and observables for the points shown in Fig. 1 with $K = K_2$ and K_3 .

$n/0.1$	$r_{\pm}/0.1$	$\lambda/10^{-5}c_-$	$n_s/0.1$	$-a_s/10^{-4}$	$r/0.01$
0.51	4.76	1.7	9.58	5.2	0.17
0.4	4.81	2	9.62	5.2	0.25
0.2	4.9	2.55	9.69	5	0.43
-0.15	5.07	3.4	9.75	4.5	0.88
-0.6	5.32	4.1	9.78	3.5	1.7
-1.5	5.88	4.5	9.78	3.98	3.7
-2.5	6.66	3.9	9.76	4	6.3
-3.2	7.35	3.3	9.73	4.4	8.3

to its upper bound in Eq. (43) and appreciably larger r values. Roughly speaking, the displayed curves can be produced interconnecting the limiting points of the various curves in Fig. 2-(a) of Ref. [23], although the curves for $0 < n < 0.1$ and $n < -0.1$ are not depicted there. This is because the r_{\pm} 's resulting from Eq. (28) are close to their upper limits induced by Eq. (25).

Comparing these theoretical outputs with data depicted by the dark [light] shaded contours at 68% c.l. [95% c.l.] we find the allowed ranges. Especially, for $K = K_1$ we obtain

$$0.62 \gtrsim n/0.1 \gtrsim -3.2, \quad 3.2 \lesssim r_{\pm}/0.1 \lesssim 4.16. \quad (45)$$

On the other hand, for $K = K_2$ or K_3 , we find one branch localized in the ranges

$$0.51 \gtrsim n/0.1 \gtrsim -0.6, \quad 4.76 \lesssim r_{\pm}/0.1 \lesssim 5.32, \quad (46)$$

and another one

$$-1.5 \gtrsim n/0.1 \gtrsim -3.2, \quad 5.88 \lesssim r_{\pm}/0.1 \lesssim 7.35. \quad (47)$$

The findings for $K = K_2$ or K_3 , can also be read-off from Table II where we list the values of the input parameter (n)

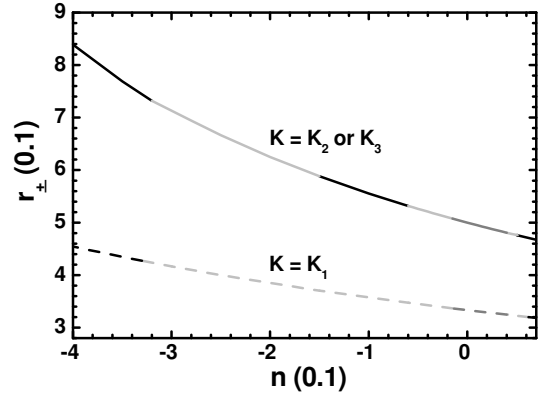


FIG. 2: Values of r_{\pm} allowed by Eq. (16) as a function of n for $K = K_1$ (dashed lines) and $K = K_2$ or K_3 (solid lines). The values which are also preferred by the observational data at 68% c.l. [95% c.l.] are included in the dark [light] gray segments.

depicted in Fig. 1, the corresponding output parameters (r_{\pm} and λ/c_-) and the inflationary observables. We observe that n_s and r are well confined in the allowed regions of Eq. (43), while a_s varies in the range $-(3.98 - 5.2) \cdot 10^{-4}$ and so, our models are consistent with the fitting of data with the Λ CDM+ r model [13]. Comparing these numerical values with those obtained by the analytic expressions in Eqs. (40a) – (40c) we obtain complete agreement for any n . On the other hand, the approximate formulas in Eqs. (41a) – (41c) are valid only for $|n_s| < 0.1$, i.e., the Starobinsky-like region. Hilltop IGHI is attained for $n > 0$ and there we find $\Delta_{\max^*} \gtrsim 0.155$, where Δ_{\max^*} increases as n drops. The required tuning is not severe, mainly for $n < 0.04$ since $\Delta_{\max^*} \gtrsim 20\%$. Since our models predict $r \gtrsim 0.0017$, they are testable by the forthcoming experiments, like BICEP3 [34], PRISM [35], LiteBIRD [36] and CORE [37], which are expected to measure r with an accuracy of 10^{-3} . We do not present in Table II ϕ_* values since, as inferred by Eq. (38), every ϕ_* satisfying Eq. (42a) leads to the same ratio λ/c_- . For the reasons mentioned below Eq. (36), we prefer $\phi_* \leq 1$. To achieve this, we need $c_- \gtrsim (30 - 140)$ for $K = K_1$ and $c_- \gtrsim (40 - 160)$ for $K = K_2$ or K_3 , where the variation of c_- is given as n decreases.

For $K = K_1$ we expect similar values for λ/c_- and the inflationary observables. However, r_{\pm} will differ appreciably due to the different relation between n and N – see Eq. (19d). To highlight it further, we present in Fig. 2 the r_{\pm} values, obtained by Eq. (28), as a function of n for $K = K_1$ (dashed lines) or $K = K_2$ and K_3 (solid lines). The values of the curves which are preferred by the observational data at 68% c.l. [95% c.l.] are included in the dark [light] gray segments – cf. Fig. 1. We observe that for tiny n values, r_{\pm} which is roughly $1/N$ lies close to $1/3$ for $K = K_1$ and $1/2$ for $K = K_2, K_3$. For larger $|n|$ values r_{\pm} deviates more drastically from these values.

The rather different predictions attained for low ($|n| \leq 0.1$) and large ($|n| > 0.1$) n values hint that the structure of \widehat{V}_{HI}

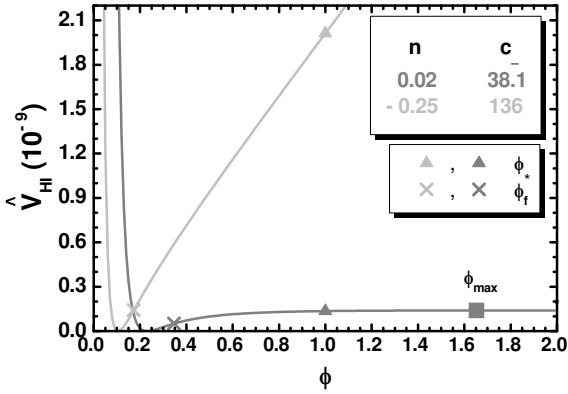


FIG. 3: The inflationary potential \widehat{V}_{HI} as a function of ϕ for $K = K_2$ or K_3 , $\phi_* = 1$ and $n = 0.02$ (gray line) or $n = -0.25$ (light gray line). The values corresponding to ϕ_* , ϕ_f and ϕ_{max} (for $n = 0.02$) are also indicated.

changes drastically. To illuminate this fact we show \widehat{V}_{HI} as a function of ϕ in Fig. 3 for $K = K_2$ or K_3 , $n = 0.02$ (gray line) and $n = -0.25$ (light gray line). We take in both cases $\phi_* = 1$. Therefore, the corresponding c_- and λ values are confined to their lowest possible values enforcing Eqs. (42a) and (42b). More specifically, we find $\lambda = 9.7 \cdot 10^{-4}$ or $5.3 \cdot 10^{-3}$ and $c_- = 38.1$ or 136 , with $M = 0.23$ or $M = 0.105$ for $n = 0.02$ or $n = -0.25$ respectively. The corresponding r_{\pm} values and observable quantities are listed in Table II. We see that in both cases \widehat{V}_{HI} develops a singularity at $\phi = 0$ contrary to the models of non-minimal inflation – cf. Ref. [20, 23] – where \widehat{V}_{HI} exhibits a maximum. However, for $n > 0$ and $|n| \sim 0.01$, \widehat{V}_{HI} resembles the potential of Starobinsky model with a maximum at $\phi_{\text{max}} = 1.65$. This does not affect much the inflationary evolution since we find $\Delta_{\text{max}*} = 39\%$, and so the tuning of the initial conditions of IGHI is rather mild. On the contrary, \widehat{V}_{HI} increases monotonically and almost linearly with ϕ for $n = -0.25$. Both behaviors can be interpreted from Eq. (20) taking into account that $f_{\text{W}} \sim \phi^2$ and $f_{\text{R}} \sim \phi^2$. For $n \sim 0.01$, $\widehat{V}_{\text{HI}} \sim f_{\text{W}}^2/f_{\text{R}}^2$ becomes more or less constant, whereas for $n \simeq -0.25$, $\widehat{V}_{\text{HI}} \sim f_{\text{W}}^2/f_{\text{R}}^{2.3/4} \sim \phi^4/\phi^3 \sim \phi$. It is also remarkable that in the latter case r increases, thanks to the increase of the inflationary scale, $\widehat{V}_{\text{HI}}^{1/4}$. Similar region of parameters is recently reported in Ref. [54].

III. A POSSIBLE POST-INFLATIONARY COMPLETION

Our discussion about IGHI is certainly incomplete without at least mentioning how the transition to the radiation dominated era is realized and the observed BAU is generated. Since these goals are related to the possible decay channels of the inflaton, the connection of IGHI with some low energy theory is unavoidable. A natural, popular and well motivated framework for particle physics at the TeV scale beyond the standard model is MSSM. A possible route to such a more complete

scenario is described in Sec. III A. Next, Sec. III B is devoted to the connection of IGHI with MSSM through the generation of the μ term. In Sec. III C, finally, we analyze the scenario of nTL exhibiting the relevant constraints and further restricting the parameters. Here and hereafter we restore units, i.e., we take $m_{\text{P}} = 2.433 \cdot 10^{18}$ GeV.

A. THE RELEVANT SET-UP

Following the post-inflationary setting of Ref. [23] we supplement the superpotential of the theory with the terms

$$W_{\text{RHN}} = \lambda_{iN^c} \bar{\Phi} N_i^{c2} + h_{Nij} N_i^c L_j H_u, \quad (48a)$$

which allows for the implementation of type I see-saw mechanism (providing masses to light neutrinos) and supports a robust baryogenesis scenario through nTL, and

$$W_{\mu} = \lambda_{\mu} S H_u H_d, \quad (48b)$$

inspired by Ref. [25], which offers a solution to one of the most tantalizing problems of MSSM, namely the generation of a μ term – for an alternative solution see Ref. [55]. Here we adopt the notation and the $B - L$ and R charges of the various superfields as displayed in Table 1 of Ref. [23]. Let us only note that L_i denotes the i -th generation $SU(2)_{\text{L}}$ doublet left-handed lepton superfields, and H_u [H_d] is the $SU(2)_{\text{L}}$ doublet Higgs superfield which couples to the up [down] quark superfields. Also, we assume that the superfields N_j^c have been rotated in the family space so that the coupling constants λ_i are real and positive. This is the so-called [3, 23] N_i^c basis, where the N_i^c masses, M_{iN^c} , are diagonal, real, and positive.

We assume that the extra fields $X^{\beta} = H_u, H_d, \tilde{N}_i^c$ have identical kinetic terms as the stabilizer field S expressed by the functions F_{lS} with $l = 1, 2, 3$ in Eqs. (5a) – (5c) – see Ref. [23]. Therefore, N_S may be renamed N_X henceforth. The inflationary trajectory in Eq. (18) has to be supplemented by the conditions

$$H_u = H_d = \tilde{N}_i^c = 0, \quad (49)$$

and the stability of this path has to be checked, parameterizing the complex fields above as we do for S in Eq. (17). The relevant masses squared are listed in Table III where we see that $\widehat{m}_{i\nu}^2 > 0$ for every ϕ . On the other hand, the positivity of the mass-squared eigenvalues $\widehat{m}_{h_{\pm}}^2$ associated with the eigenstates \widehat{h}_{\pm} and \widehat{h}_{\pm} , where

$$\widehat{h}_{\pm} = (\widehat{h}_u \pm \widehat{h}_d)/\sqrt{2} \quad \text{and} \quad \widehat{h}_{\pm} = (\widehat{h}_u \pm \widehat{h}_d)/\sqrt{2}, \quad (50)$$

requires the establishment of the inequalities

$$\lambda_{\mu} \lesssim \lambda f_{\text{W}}(1 + f_{\text{W}}/N)/4\lambda_{\mu} c_+^2 \phi^2 \quad \text{for } K = K_1; \quad (51a)$$

$$\lambda_{\mu} \lesssim \lambda f_{\text{W}}(1 + 1/N_X)/4c_+ \quad \text{for } K = K_2, K_3. \quad (51b)$$

In both cases, the inequalities are fulfilled for $\lambda_{\mu} \lesssim 2 \cdot 10^{-5}$. Similar numbers are obtained in Ref. [3, 23]. We do not

TABLE III: Mass-squared spectrum of the non-inflaton sector along the path in Eqs. (18) and (49).

FIELDS	EIGEN-STATES	MASSES SQUARED			
			$K = K_1$	$K = K_2$	$K = K_3$
10 Real Scalars	$\widehat{h}_\pm, \widehat{\bar{h}}_\pm$	$\widehat{m}_{h_\pm}^2$	$3\widehat{H}_{\text{HI}}^2 (1 + f_W/N \pm 4\lambda_\mu c_+^2 \phi^2 / \lambda f_W)$	$3\widehat{H}_{\text{HI}}^2 (1 + 1/N_X \pm 4\lambda_\mu c_+ / \lambda f_W)$	
	$\widehat{\nu}_i^c, \widehat{\bar{\nu}}_i^c$	$\widehat{m}_{\bar{\nu}^c}^2$	$3\widehat{H}_{\text{HI}}^2 ((1 + f_W/N)/c_+ \phi^2 + 16\lambda_{iN^c}^2 c_+^2 \phi^2 / \lambda^2 f_W^2)$	$3\widehat{H}_{\text{HI}}^2 (1 + 1/N_X + 16\lambda_{iN^c}^2 c_+^2 \phi^2 / \lambda^2 f_W^2)$	
3 Weyl Spinors	\widehat{N}_i^c	$m_{iN^c}^2$	$48\lambda_{iN^c}^2 c_+^2 \phi^2 \widehat{H}_{\text{HI}}^2 / \lambda^2 f_W^2$		

consider such a condition on λ_μ as unnatural, given that the Yukawa coupling constant h_{1U} , which provides masses to the up-type quarks, is of the same order of magnitude too at a high scale – cf. Ref. [56]. Note that the hierarchy in Eqs. (51a) and (51b) between λ_μ and λ differs from that imposed in the models [25] of F-term hybrid inflation, where S plays the role of inflaton and $\Phi, \bar{\Phi}, H_u$ and H_d are confined at zero. Indeed, in that case we demand [25] $\lambda_\mu > \lambda$ so that the tachyonic instability in the $\Phi - \bar{\Phi}$ direction occurs first, and the $\Phi - \bar{\Phi}$ system start evolving towards its v.e.v, whereas H_u and H_d continue to be confined to zero. In our case, though, the inflaton is included in the $\bar{\Phi} - \Phi$ system while S and the $H_u - H_d$ system are safely stabilized at the origin both during and after IGHI. Therefore, ϕ settles in its vacuum and S, H_u and H_d take their non-vanishing electroweak scale v.e.v.s afterwards.

B. A SOLUTION TO THE μ PROBLEM OF MSSM

A byproduct of the R symmetry associated with our models is that it assists us to understand the origin of the μ term of MSSM – see Sec. III B 1 – connecting thereby the high with the low energy phenomenology as described in Sec. III B 2.

1. Generating the μ Parameter

Working along the lines of Sec. II A 2 we can verify that the presence of the terms in Eqs. (48a) and (48b) leave the v.e.v.s in Eq. (15) unaltered whereas those of X^β are found to be

$$\langle H_u \rangle = \langle H_d \rangle = \langle \widetilde{N}_i^c \rangle = 0. \quad (52)$$

On the other hand, the contributions from the soft SUSY breaking terms, although negligible during IGHI – since these are expected to be much smaller than $\phi -$, may slightly shift [3, 23, 25] $\langle S \rangle$ from zero in Eq. (15). Indeed, the relevant potential terms are

$$V_{\text{soft}} = (\lambda A_\lambda S \bar{\Phi} \Phi - a_S S \lambda M^2 / 4 + \text{h.c.}) + m_\gamma^2 |X^\gamma|^2, \quad (53)$$

where $X^\gamma = \Phi, \bar{\Phi}, S, H_u, H_d, \widetilde{N}_i^c$, and m_γ, A_λ and a_S are soft SUSY breaking mass parameters of the order of TeV. The emergence of these terms depend on the mechanism of SUSY breaking which is not specified here. We restrict ourselves to assume that this extra sector of the theory may be included in the present set-up without disturbing the status of inflation – cf. Ref. [57].

Confining $\Phi, \bar{\Phi}, H_u, H_d$ and N_i^c in their v.e.v.s in Eqs. (15) and (52), \widehat{V} in Eq. (6b) reduces again to V_{eff} in Eq. (11a) with vanishing terms represented by ellipsis since $\langle W_{\text{HI}} \rangle = 0$. Rotating S to the real axis by an appropriate R -transformation and choosing conveniently the phases of A_λ and a_S so as the total low-energy potential

$$V_{\text{tot}} = V_{\text{eff}} + V_{\text{soft}} \quad (54)$$

to be minimized, we obtain for $K = K_2$ or K_3

$$\langle V_{\text{tot}}(S) \rangle \simeq \frac{\lambda^2 S^2}{2 \langle \det M_\pm \rangle} (c_- M^2 - N m_P^2) - \lambda a_{3/2} m_{3/2} M^2 S, \quad (55a)$$

where the first term in the r.h.s originates from the second line of Eq. (14) for $e^{\widetilde{K} + m_P^2} \simeq 1$, and Φ and $\bar{\Phi}$ equal to their v.e.v.s in Eq. (15). Also, we take into account that $m_S \ll M$, and we set

$$|A_\lambda| + |a_S| = 2a_{3/2} m_{3/2}, \quad (55b)$$

where $m_{3/2}$ is the \widetilde{G} mass and $a_{3/2} > 0$ a parameter of order unity which parameterizes our ignorance of the dependence of $|A_\lambda|$ and $|a_S|$ on $m_{3/2}$. The minimization condition for the total potential in Eq. (55a) w.r.t S leads to a non vanishing $\langle S \rangle$ as follows

$$\frac{d}{dS} \langle V_{\text{tot}}(S) \rangle = 0 \Rightarrow \langle S \rangle \simeq a_{3/2} m_{3/2} c_- (1 + N r_\pm) / \lambda, \quad (55c)$$

since from Eqs. (13c), (15) and (16) we infer

$$\langle \det M_\pm \rangle = c_-^2 - N^2 c_+^2 = c_-^2 (1 + N r_\pm) (1 - N r_\pm). \quad (55d)$$

At this S value, $\langle V_{\text{tot}}(S) \rangle$ develops a minimum since

$$\frac{d^2}{dS^2} \langle V_{\text{tot}}(S) \rangle = \lambda^2 / c_+ (c_- + N c_+) > 0. \quad (55e)$$

For $K = K_1$ Eq. (55c) can be obtained again by doing an expansion of the relevant expressions in powers $1/m_P$.

The μ term generated from Eq. (48b) exhibits the mixing parameter

$$\mu = \lambda_\mu \langle S \rangle \simeq \lambda_\mu a_{3/2} m_{3/2} c_- (1 + N r_\pm) / \lambda. \quad (56a)$$

Comparing this result with the corresponding one in Ref. [23], we deduce a crucial difference regarding the sign of the expression in the parenthesis which originates from the terms in

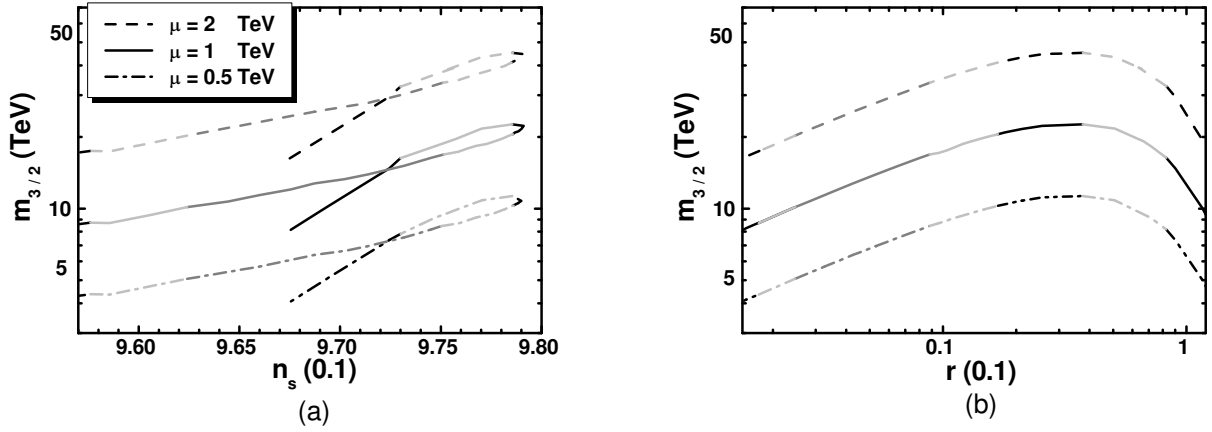


FIG. 4: The gravitino mass $m_{3/2}$ versus n_s (a) and r (b) for $\lambda_\mu = 10^{-6}$, $a_{3/2} = 1$, $K = K_2$ or K_3 with $N_X = 2$ and $\mu = 0.5$ TeV (dot-dashed line), $\mu = 1$ TeV (solid line), or $\mu = 2$ TeV (dashed line). The color coding is as in Fig. 2.

the second line of Eq. (14). With the aid of Eq. (38) we may eliminate c_- and λ from the above result which then reads

$$\mu \simeq 1.2 \cdot 10^2 \lambda_\mu \frac{a_{3/2} m_{3/2} (1 + N r_\pm) (f_{\mathcal{R}^*} - 1)^2}{r_\pm^{3/2} f_{\mathcal{R}^*}^{n+1/2} (n(1 - f_{\mathcal{R}^*}) + 1)}, \quad (56b)$$

where Eq. (42b) is employed to obtain the numerical prefactor. Taking into account Eqs. (28) and (34), we infer that the resulting μ depends only on n and not on λ , c_- and r_\pm – cf. Ref. [23, 25]. For the λ_μ values allowed by Eqs. (51a) and (51b), any $|\mu|$ value is accessible with a mild hierarchy between $m_{3/2}$ and μ – from Table III we see that both signs of λ_μ (and so μ) are possible without altering the stability analysis of the inflationary system. To understand this, let us first remark that Eq. (16) implies $r_\pm \simeq 1/N$ and $f_{\mathcal{R}^*}$ varies from about 12 to 68 [15 to 119] for $K = K_1$ [$K = K_2$ and K_3], as n varies in the allowed ranges of Eqs. (45) – (47). A rough estimation gives $\mu \sim 10^2 \lambda_\mu f_{\mathcal{R}^*}^{3/2} = 10^{-1.5} m_{3/2}$ and so we expect that μ is about one order of magnitude less than $m_{3/2}$.

To highlight further the conclusions above, we can employ Eq. (56a) to derive the $m_{3/2}$ values required so as to obtain a specific μ value. Given that Eq. (56a) depends on n , which crucially influences n_s and r , we expect that the required $m_{3/2}$ is a function of n_s and r as depicted in Fig. 4-(a) and Fig. 4-(b) respectively. We take $\lambda_\mu = 10^{-6}$, in accordance with Eqs. (51a) and (51b), $a_{3/2} = 1$, $K = K_2$ or K_3 with $N_X = 2$ and $\mu = 0.5$ TeV (dot-dashed line), $\mu = 1$ TeV (solid line), or $\mu = 2$ TeV (dashed line). Varying n in the allowed range indicated in Fig. 1-(a) we obtain the variation of $m_{3/2}$ solving Eq. (56a) w.r.t $m_{3/2}$. The values of the curves which are preferred by the observational data at 68% c.l. [95% c.l.] are included in the dark [light] gray segments – cf. Fig. 1. We see that $m_{3/2}$ increases with μ and its lowest value $m_{3/2} \simeq 4$ TeV is obtained for $\mu = 0.5$ TeV. As we anticipated above, $m_{3/2}$ is almost one order of magnitude larger than the corresponding μ . Moreover, for fixed μ , each curve develops a maximum at $n \simeq -0.15$, which coincides with the right corner of the curve in Fig. 1. This behavior deviates a lot from the one found in Ref. [23] and comes from the different sign in the parenthesis of Eq. (56a).

2. Connection with the Parameters of CMSSM

The SUSY breaking effects, considered in Eq. (53), explicitly break $U(1)_R$ to a subgroup, \mathbb{Z}_2^R which can be identified with a matter parity. Under this discrete symmetry all the matter (quark and lepton) superfields change sign – see Table 1 of Ref. [23]. Since S has the R symmetry of W , $\langle S \rangle$ in Eq. (55c) also breaks spontaneously $U(1)_R$ to \mathbb{Z}_2^R . Thanks to this fact, \mathbb{Z}_2^R remains unbroken and so no disastrous domain walls are formed. Combining \mathbb{Z}_2^R with the \mathbb{Z}_2^f fermion parity, under which all fermions change sign, yields the well-known R -parity. This residual symmetry prevents rapid proton decay and guarantees the stability of the *lightest SUSY particle* (LSP), providing thereby a well-motivated *cold dark matter* (CDM) candidate.

The candidacy of LSP may be successful, if it generates the correct CDM abundance [53] within a concrete low energy framework, which in our case is the MSSM or one of its variants. Here, we adopt the *Constrained MSSM* (CMSSM) which is the most restrictive, predictive and well-motivated version of MSSM, employing the free parameters

$$\text{sign}\mu, \quad \tan\beta = \langle H_u \rangle / \langle H_d \rangle, \quad M_{1/2}, \quad m_0, \quad \text{and} \quad A_0,$$

where $\text{sign}\mu$ is the sign of μ , and the three last mass parameters denote the common gaugino mass, scalar mass and trilinear coupling constant, respectively, defined (normally) at M_{GUT} . The parameter $|\mu|$ is not free, since it is computed at low scale by enforcing the conditions for the electroweak symmetry breaking. The values of these parameters can be tightly restricted imposing a number of cosmological constraints from which the consistency of LSP relic density with observations plays a central role. Some updated results are recently presented in Ref. [58], where we can also find the best-fit values of $|A_0|$, m_0 and $|\mu|$ listed in the first four lines of Table IV. We see that there are four allowed regions characterized by the mechanism applied for accommodating an acceptable LSP relic density.

Taking advantage of this investigation, we can check whether the μ and $m_{3/2}$ values satisfying Eq. (56a) are consis-

TABLE IV: The required λ_μ values rendering our models compatible with the best-fit points of the CMSSM as found in Ref. [58] with the assumptions in Eq. (57).

CMSSM REGION:	A/H FUNNEL	$\tilde{\tau}_1 - \chi$			$\tilde{t}_1 - \chi$			$\tilde{\chi}_1^\pm - \chi$		
		COANNIHILATION								
$ A_0 $ (TeV)	9.924	1.227	9.965	9.2061						
m_0 (TeV)	9.136	1.476	4.269	9.000						
$ \mu $ (TeV)	1.409	2.62	4.073	0.983						
$a_{3/2}$	1.086	0.831	2.33	1.023						
$\lambda_\mu(10^{-6})$ for $K = K_1$										
$n = 0.02$	1.409	<i>21.19</i>	4.063	1.059						
$n = -0.25$	1.87	28.11	5.39	1.405						
$\lambda_\mu(10^{-6})$ for $K = K_2$ and K_3										
$n = 0.02$	1.814	<i>27.28</i>	5.23	1.363						
$n = -0.25$	2.784	<i>41.86</i>	8.025	2.092						

tent with these values. Selecting some representative n values and adopting the identifications

$$m_0 = m_{3/2} \quad \text{and} \quad |A_\lambda| = |a_S| = |A_0|, \quad (57)$$

we can first derive $a_{3/2}$ from Eq. (55b) and then the λ_μ values from Eq. (56a), which yield the phenomenologically desired $|\mu|$ shown in the third line of Table IV. Here we assume that renormalization effects in the derivation of μ are negligible. The outputs of our computation are assembled in the last six lines of Table IV. As inputs, we take $n = 0.02$ and -0.25 which are central values in the two regions compatible with the inflationary observations as found in Sec. II C 2. From the outputs we infer that the required λ_μ values are comfortably compatible with Eqs. (51a) and (51b) for $N_X = 2$, in all cases besides the one corresponding to the $\tilde{\tau}_1 - \chi$ coannihilation region. In that case, m_0 is lower than $|\mu|$ and so marginally large λ_μ values are required. In the cases where numbers are written in italics, we obtain instability along the inflationary path for $K = K_1$, whereas for $K = K_2$ and K_3 we need $0 \leq N_X \leq 1$ to avoid this effect. Note that the λ_μ values found here are larger compared to those found in Refs. [3, 23]. Moreover, in sharp contrast to the model of Ref. [23], only the A/H funnel and $\tilde{\chi}_1^\pm - \chi$ coannihilation regions can be consistent with the \tilde{G} limit on T_{rh} – see Sec. III C 2. Indeed, $m_{3/2} \gtrsim 9$ TeV become cosmologically safe under the assumption of an unstable \tilde{G} , for the T_{rh} values necessitated for satisfactory leptogenesis – see Sec. III C 3.

C. NON-THERMAL LEPTOGENESIS

Our next task is to specify how our inflationary scenario makes a transition to the radiation dominated era – see Sec. III C 1 – and offers an explanation of the observed BAU consistent with the \tilde{G} constraint and the low energy neutrino data – see Sec. III C 2. Our results are summarized in Sec. III C 3.

1. Inflaton Mass and Decay

When IGHI is over, the inflaton continues to roll down towards the SUSY vacuum, Eq. (15). Soon after, it settles into a phase of damped oscillations around the minimum of \hat{V}_{HI} . The (canonically normalized) inflaton,

$$\widehat{\delta\phi} = \langle J \rangle \delta\phi \quad \text{with} \quad \delta\phi = \phi - M, \quad (58)$$

and

$$\langle J \rangle = \sqrt{\langle \kappa_+ \rangle} = \sqrt{c_- (1 + N r_\pm)}, \quad (59)$$

acquires mass, at the SUSY vacuum in Eq. (15), which is given by

$$\widehat{m}_{\delta\phi} = \left\langle \widehat{V}_{\text{HI}, \widehat{\phi\phi}} \right\rangle^{1/2} = \frac{\lambda m_{\text{P}}}{\sqrt{2c_+ \langle J \rangle}} = \frac{\lambda m_{\text{P}}}{c_- \sqrt{2(1 + N r_\pm)}}. \quad (60)$$

From the last expression we can infer that $\widehat{m}_{\delta\phi}$ remains constant for fixed n since λ/c_- is fixed too – see Eq. (38). In particular, for $K = K_1$ and the allowed range of n in Eq. (45) we obtain

$$2.9 \lesssim \widehat{m}_{\delta\phi}/10^{13} \text{ GeV} \lesssim 5. \quad (61a)$$

For $K = K_2$ and K_3 , in the allowed ranges of Eqs. (46) and (47), we obtain

$$3.1 \lesssim \widehat{m}_{\delta\phi}/10^{13} \text{ GeV} \lesssim 6.9; \quad (61b)$$

$$4.1 \lesssim \widehat{m}_{\delta\phi}/10^{13} \text{ GeV} \lesssim 7.2. \quad (61c)$$

We remark that $\widehat{m}_{\delta\phi}$ is somewhat affected by the choice of K 's in Eqs. (3a) – (3c). For $n = 0$, $\widehat{m}_{\delta\phi} = 4.7 \cdot 10^{13}$ GeV for $K = K_1$, and $\widehat{m}_{\delta\phi} = 5.2 \cdot 10^{13}$ GeV for $K = K_2$ and K_3 , which are both somewhat larger than the value obtained within Starobinsky inflation [3, 6]. On the other hand, these values are close to the maximal ones found in Ref. [23], since here r_\pm approaches its maximal value.

The inflaton can decay [59] perturbatively into:

(a) A pair of N_i^c with Majorana masses $M_{iN^c} = \lambda_{iN^c} M$ with the decay width

$$\widehat{\Gamma}_{\delta\phi \rightarrow N_i^c N_i^c} = \frac{g_{iN^c}^2}{16\pi} \widehat{m}_{\delta\phi} \left(1 - \frac{4M_{iN^c}^2}{\widehat{m}_{\delta\phi}^2} \right)^{3/2}, \quad (62a)$$

where the relevant coupling constant

$$g_{iN^c} = (N-1) \frac{\lambda_{iN^c}}{\langle J \rangle} = \frac{(N-1) r_\pm^{1/2}}{(1 + N r_\pm)^{1/2}} \frac{M_{iN^c}}{m_{\text{P}}} \quad (62b)$$

arises from from the lagrangian term

$$\begin{aligned} \mathcal{L}_{\widehat{\delta\phi} \rightarrow N_i^c N_i^c} &= -\frac{1}{2} e^{K/2m_{\text{P}}^2} W_{\text{HI}, N_i^c N_i^c} N_i^c N_i^c + \text{h.c.} \\ &= g_{iN^c} \widehat{\delta\phi} N_i^c N_i^c + \text{h.c.} \end{aligned} \quad (62c)$$

This decay channel activates the mechanism of nTL, as sketched in Sec. III C 2.

(b) Higgses H_u and H_d with the decay width

$$\widehat{\Gamma}_{\delta\phi \rightarrow H_u H_d} = \frac{2}{8\pi} g_H^2 \widehat{m}_{\delta\phi} \quad \text{where} \quad g_H = \frac{\lambda_\mu}{\sqrt{2}}, \quad (63a)$$

arises from the lagrangian term

$$\begin{aligned} \mathcal{L}_{\widehat{\delta\phi} \rightarrow H_u H_d} &= -e^{K/m_{\text{P}}^2} K^{SS^*} |W_{\text{HI},S}|^2 \\ &= -g_H \widehat{m}_{\delta\phi} \widehat{\delta\phi} (H_u^* H_d^* + \text{h.c.}) + \dots \end{aligned} \quad (63b)$$

Thanks to the upper bounds on λ_μ from Eqs. (51a) and (51b), g_H turns out to be comparable with g_{iN^c} .

(c) MSSM (s)-particles XYZ with the following c_+ -dependent 3-body decay width

$$\widehat{\Gamma}_{\delta\phi \rightarrow XYZ} = g_y^2 \frac{14n_f}{512\pi^3} \frac{\widehat{m}_{\delta\phi}^3}{m_{\text{P}}^2}, \quad (64a)$$

where for the third generation we take $y \simeq (0.4 - 0.6)$, computed at the $\widehat{m}_{\delta\phi}$ scale, and $n_f = 14$ for $\widehat{m}_{\delta\phi} < M_{3N^c}$. Also,

$$g_y = N y_3 \sqrt{\frac{r_\pm}{1 + N r_\pm}}, \quad (64b)$$

and $y_3 = h_{t,b,\tau}(\widehat{m}_{\delta\phi}) \simeq 0.5$. Since $r_\pm \simeq 1/N$ we can easily infer that g_y above is enhanced compared to the corresponding one in Ref. [23] where $r_\pm \simeq 0.01$, and an additional suppression through a ratio M/m_{P} exists. We therefore expect that $\widehat{\Gamma}_{\delta\phi \rightarrow XYZ}$ contributes sizably to the total decay width of $\widehat{\delta\phi}$. Each individual decay width arises from the lagrangian terms

$$\begin{aligned} \mathcal{L}_{\widehat{\delta\phi} \rightarrow X\psi_Y\psi_Z} &= -\frac{1}{2} e^{K/2m_{\text{P}}^2} (W_{y,YZ}\psi_Y\psi_Z) + \text{h.c.} \\ &= -\lambda_y \frac{\widehat{\delta\phi}}{m_{\text{P}}} (X\psi_Y\psi_Z) + \text{h.c.}, \end{aligned} \quad (64c)$$

where $W_y = yXYZ$ is a typical trilinear superpotential term of MSSM with y a Yukawa coupling constant, and ψ_X, ψ_Y and ψ_Z are the chiral fermions associated with the superfields X, Y and Z whose scalar components are denoted with the superfield symbols.

The resulting reheat temperature is given by [60]

$$T_{\text{rh}} = (72/5\pi^2 g_*)^{1/4} \widehat{\Gamma}_{\delta\phi}^{1/2} m_{\text{P}}^{1/2}, \quad (65a)$$

with the total decay width of $\widehat{\delta\phi}$ being

$$\widehat{\Gamma}_{\delta\phi} = \widehat{\Gamma}_{\delta\phi \rightarrow N_i^c N_i^c} + \widehat{\Gamma}_{\delta\phi \rightarrow H_u H_d} + \widehat{\Gamma}_{\delta\phi \rightarrow XYZ}. \quad (65b)$$

Here, $g_* = 228.75$ counts the MSSM effective number of relativistic degrees of freedom at temperature T_{rh} .

2. Lepton-Number and Gravitino Abundances

For $T_{\text{rh}} < M_{iN^c}$, the out-of-equilibrium decay of ν_i^c generates a lepton-number asymmetry (per ν_i^c decay), ε_i – see,

e.g., Ref. [38, 39]. The resulting ε_i is partially converted through sphaleron effects into a yield of the observed BAU [23, 38, 39],

$$Y_B = -0.35 \cdot 2 \cdot \frac{5}{4} \frac{T_{\text{rh}}}{\widehat{m}_{\delta\phi}} \sum_i \frac{\widehat{\Gamma}_{\delta\phi \rightarrow N_i^c N_i^c}}{\widehat{\Gamma}_{\delta\phi}} \varepsilon_i, \quad (66)$$

which has to reproduce the observational result [53]:

$$Y_B = (8.64_{-0.16}^{+0.15}) \cdot 10^{-11}. \quad (67)$$

The validity of Eq. (66) requires that the $\widehat{\delta\phi}$ decay into a pair of N_i^c 's is kinematically allowed for at least one species of the N_i^c 's and also that there is no erasure of the produced Y_L due to N_1^c mediated inverse decays and $\Delta L = 1$ scatterings [62]. These prerequisites are ensured if we impose

$$(a) \widehat{m}_{\delta\phi} \geq 2M_{1N^c} \quad \text{and} \quad (b) M_{1N^c} \gtrsim 10T_{\text{rh}}. \quad (68)$$

The quantity ε_i can be expressed in terms of the Dirac masses of ν_i , m_{iD} , arising from the second term of Eq. (48a) – see Ref. [23]. Moreover, employing the seesaw formula we can then obtain the light-neutrino mass matrix m_ν in terms of m_{iD} and M_{iN^c} . As a consequence, nTL can be nicely linked to low energy neutrino data. We take as inputs the best-fit values [44] – see also Ref. [45] – of the neutrino mass-squared differences, $\Delta m_{21}^2 = 7.6 \cdot 10^{-5} \text{ eV}^2$ and $\Delta m_{31}^2 = (2.48 [-2.38]) \cdot 10^{-3} \text{ eV}^2$, of the mixing angles, $\sin^2 \theta_{12} = 0.323$, $\sin^2 \theta_{13} = 0.0226$ [$\sin^2 \theta_{13} = 0.029$] and $\sin^2 \theta_{23} = 0.567$ [$\sin^2 \theta_{23} = 0.573$], and of the CP-violating Dirac phase $\delta = 1.41\pi$ [$\delta = 1.48\pi$] for *normal* [*inverted*] *ordered* (NO [IO]) *neutrino masses*, $m_{i\nu}$'s. The sum of $m_{i\nu}$'s is bounded from above by the data [53],

$$\sum_i m_{i\nu} \leq 0.23 \text{ eV} \quad (69)$$

at 95% c.l. This is more restrictive than the 90% c.l. upper bound arising from the effective electron neutrino mass in β -decay [63]:

$$m_\beta \leq (0.061 - 0.165) \text{ eV}, \quad (70)$$

where the range accounts for nuclear matrix element uncertainties.

The required T_{rh} in Eq. (66) must be compatible with constraints on the \widetilde{G} abundance, $Y_{3/2}$, at the onset of *nucleosynthesis* (BBN), which are [42] given approximately by

$$Y_{3/2} \lesssim \begin{cases} 10^{-14} \\ 10^{-13} \\ 10^{-12} \end{cases} \quad \text{for} \quad m_{3/2} \simeq \begin{cases} 0.69 \text{ TeV}, \\ 10.6 \text{ TeV}, \\ 13.5 \text{ TeV}. \end{cases} \quad (71)$$

Here we consider the conservative case where \widetilde{G} decays with a tiny hadronic branching ratio. The bounds above can be somehow relaxed in the case of a stable \widetilde{G} – see e.g. Ref. [28].

In our models $Y_{3/2}$ is estimated to be [41, 42]:

$$Y_{3/2} \simeq 1.9 \cdot 10^{-22} T_{\text{rh}}/\text{GeV}, \quad (72)$$

where we take into account only thermal production of \tilde{G} , and assume that \tilde{G} is much heavier than the MSSM gauginos. Non-thermal contributions to $Y_{3/2}$ [59] are also possible but strongly dependent on the mechanism of soft SUSY breaking. Moreover, no precise computation of this contribution exists within IGHI adopting the simplest Polonyi model of SUSY breaking [43]. It is notable, though, that the non-thermal contribution to $Y_{3/2}$ in models with stabilizer field, as in our case, is significantly suppressed compared to the thermal one.

3. Results

It is worthwhile to test the applicability of the framework above in the case of IGHI. Namely, following a bottom-up approach detailed in Ref. [23], we find the M_{iN^c} 's by using as inputs the m_{iD} 's, a reference mass of the ν_i 's – $m_{1\nu}$ for NO $m_{i\nu}$'s, or $m_{3\nu}$ for IO $m_{i\nu}$'s –, the two Majorana phases φ_1 and φ_2 of the PMNS matrix, and the best-fit values, mentioned in Sec. III C 2, for the low energy parameters of neutrino physics – note that there are no experimental constraints on φ_1 and φ_2 up to now. In our numerical code we also estimate, following Ref. [61], the renormalization group evolved values of the latter parameters at the scale of nTL, $\Lambda_L = \hat{m}_{\delta\phi}$, by considering the MSSM with $\tan\beta \simeq 50$ as an effective theory between Λ_L and the soft SUSY breaking scale, $M_{\text{SUSY}} = 1.5$ TeV. We evaluate the M_{iN^c} 's at Λ_L , and we neglect any possible running of the m_{iD} 's and M_{iN^c} 's. Therefore, we present their values at Λ_L .

We start the exposition of our results arranging in Table V some representative values of the parameters which yield Y_B and $Y_{3/2}$ compatible with Eqs. (67) and (71), respectively. Throughout our computation we take $\lambda_\mu = 10^{-6}$, in accordance with Eqs. (51a) and (51b), and $y = 0.5$, which is a typical value encountered [56] in various MSSM settings with large $\tan\beta$. Also, we select $n = 0.02$ which yields n and r in the “sweet” spot of the present data – see Fig. 1. We obtain $M = 6.1 \cdot 10^{17}$ GeV and $\hat{m}_{\delta\phi} = 4.2 \cdot 10^{13}$ GeV for $K = K_1$, or $M = 5.6 \cdot 10^{15}$ GeV and $\hat{m}_{\delta\phi} = 4.4 \cdot 10^{13}$ GeV for $K = K_2$ or K_3 . Although the uncertainties from the choice of K 's are negligible as regards the quantities above, the decay widths in Sec. III C 1 depend on N and r_\pm which take different values for $K = K_1$ and $K = K_2$ or K_3 – see Fig. 2 – discriminating somehow the two choices. For this reason, we clarify that we adopt $K = K_2$ or K_3 with $N_X = 2$ for the bulk of the computation below. Had we employed $K = K_1$, we would have obtained almost two times larger Y_B 's with the same values of the free parameters. Therefore a mild readjustment is needed.

In Table V we consider NO (cases A and B), almost degenerate (cases C, D and E) and IO (cases F and G) $m_{i\nu}$'s. In all cases Eq. (69) is safely met – the case D saturates it – whereas Eq. (70) is comfortably satisfied. The gauge group adopted here, G_{B-L} , does not predict any relation between the Yukawa couplings constants h_{iN} entering the second term of Eq. (48a) and the other Yukawa couplings in the MSSM. As a consequence, the m_{iD} 's are free parameters. However, for the sake of comparison, for cases A – F, we take $m_{3D} = m_t(\Lambda_L) \simeq 100$ GeV, where m_t denotes the mass of

TABLE V: Parameters yielding the correct BAU for $K = K_2$ or K_3 , $n = 0.02$, $\lambda_\mu = 10^{-6}$, $y_3 = 0.5$ and various neutrino mass schemes.

PARAMETERS	CASES						
	A	B	C	D	E	F	G
	Normal Hierarchy		Almost Degeneracy			Inverted Hierarchy	
Low Scale Parameters (Masses in eV)							
$m_{1\nu}/0.1$	0.01	0.1	0.5	0.7	0.7	0.5	0.49
$m_{2\nu}/0.1$	0.09	0.13	0.51	1.0	0.705	0.51	0.5
$m_{3\nu}/0.1$	0.5	0.51	0.71	1.12	0.5	0.1	0.05
$\sum_i m_{i\nu}/0.1$	0.6	0.74	1.7	2.3	1.9	1.1	1
$m_\beta/0.01$	0.22	0.98	3.5	5.3	2.9	4.9	3.6
φ_1	0	0	0	$\pi/2$	$\pi/2$	$-3\pi/4$	0
φ_2	$-\pi/2$	0	$\pi/2$	$-\pi$	$-2\pi/3$	$5\pi/4$	$-\pi/2$
Leptogenesis-Scale Mass Parameters in GeV							
m_{1D}	1.98	1.5	2.3	4.16	5.2	1	6.3
m_{2D}	38	16.6	12	10	9.6	6.6	10
$m_{3D}/100$	1	1	1	1	1	1	0.33
$M_{1N^c}/10^{11}$	1.6	2.1	1.4	2.8	5.2	0.2	8.9
$M_{2N^c}/10^{12}$	27	6.8	2.6	4.8	1.9	2.2	3.2
$M_{3N^c}/10^{14}$	22	4.7	0.89	0.22	0.69	2.9	0.9
Decay channels of the Inflaton $\hat{\delta\phi}$							
$\hat{\delta\phi} \rightarrow$	N_1^c	$N_{1,2}^c$	$N_{1,2}^c$	$N_{1,2}^c$	$N_{1,2}^c$	$N_{1,2}^c$	$N_{1,2}^c$
Resulting B -Yield							
$Y_B^0/10^{-11}$	9.63	8	8.4	9.1	8.9	8.7	8.9
$Y_B/10^{-11}$	8.67	8.59	8.69	8.56	8.65	8.67	8.65
Resulting T_{rh} (in GeV) and \tilde{G} -Yield							
$T_{\text{rh}}/10^9$	1	1.1	1	1.1	1	1	1
$10^{13}Y_{3/2}$	1.91	2.2	1.9	2	1.9	1.9	1.97

the top quark. Similar conditions for the lighter generations do not hold, though, in our data sample.

Besides case A, where only the channel $\hat{\delta\phi} \rightarrow N_1^c N_1^c$ is kinematically unblocked, $\hat{\delta\phi}$ decays into N_1^c 's and N_2^c 's. In the latter cases ε_2 yields the dominant contribution to the calculation Y_B from Eq. (66). From our computation, we also remark that $\hat{\Gamma}_{\delta\phi \rightarrow N_i^c N_i^c} < \hat{\Gamma}_{\delta\phi \rightarrow H_u H_d} < \hat{\Gamma}_{\delta\phi \rightarrow XYZ}$, and so the ratios $\hat{\Gamma}_{\delta\phi \rightarrow N_i^c N_i^c} / \hat{\Gamma}_{\delta\phi}$ introduce a considerable reduction (0.02 – 0.25) in the derivation of Y_B . As a consequence, the attainment of the correct Y_B requires relatively large m_{iD} 's with $i = 1, 2$ in order to achieve sizable enough $\hat{\Gamma}_{\delta\phi \rightarrow N_i^c N_i^c}$. Namely, $m_{1D} \gtrsim 1$ GeV and $m_{2D} \gtrsim 6.6$ GeV. Besides case A, the first inequality is necessary, in order to fulfill the second inequality in Eq. (68), given that m_{1D} heavily influences M_{1N^c} . In Table V we also display, for comparison, the B -yield with (Y_B) or without (Y_B^0) taking into account the renor-

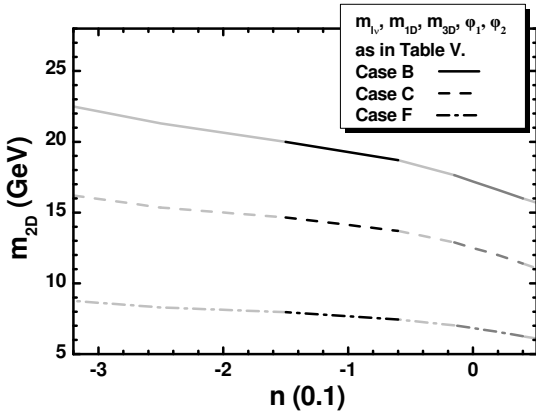


FIG. 5: Contours in the $n - m_{2D}$ plane yielding the central Y_B in Eq. (67) consistently with the inflationary requirements for $K = K_2$ or K_3 , $\lambda_\mu = 10^{-6}$, $y_3 = 0.5$ and the values of $m_{i\nu}$, m_{1D} , m_{3D} , φ_1 , and φ_2 which correspond to the cases B (solid line), C (dashed line), and F (dot-dashed line) of Table V. The color coding is as in Fig. 2.

malization group effects. We observe that the two results are mostly close to each other. Shown also are values for T_{rh} , the majority of which are close to 10^9 GeV, and the corresponding $Y_{3/2}$'s, which are consistent with Eq. (71) mostly for $m_{3/2} \gtrsim 10$ TeV. These large values can be marginally tolerated with the $m_{3/2}$'s appearing in Table IV and Figs. 2 and 3 of Ref. [58] in the A/H funnel and $\tilde{\chi}_1^\pm - \chi$ coannihilation regions – see also Ref. [64]. These $m_{3/2}$'s though are more easily reconciled with low energy data in versions of MSSM less restrictive than CMSSM – see Ref. [65].

In order to extend the conclusions inferred from Table V to the case of variable n , we can examine how the central value of Y_B in Eq. (67) can be achieved by varying m_{2D} as a function of n . The resulting contours in the $n - m_{2D}$ plane are presented in Fig. 5 – since the range of Y_B in Eq. (67) is very narrow, the 95% c.l. width of these contours is negligible. The convention adopted for these lines is also described in the figure. In particular, we use solid, dashed, or dot-dashed line for $m_{i\nu}$, m_{1D} , m_{3D} , φ_1 , and φ_2 corresponding to the cases B, D, or F of Table V respectively. For n within its allowed margins in Eqs. (46) and (47) we obtain $0.4 \lesssim T_{\text{rh}}/10^9 \text{ GeV} \lesssim 1.8$, which is perfectly acceptable from Eq. (71) for $m_{3/2} \gtrsim 10$ TeV. Along the depicted contours, the resulting M_{2N^c} 's vary in the ranges $(5.7 - 14.5) \cdot 10^{12}$ GeV, $(1.8 - 4.6) \cdot 10^{12}$ GeV, $(1.5 - 3.9) \cdot 10^{12}$ GeV for cases B, C and F respectively, whereas M_{1N^c} and M_{3N^c} remain close to their values presented in the corresponding cases of Table III.

Comparing, finally, our results above with those presented in Ref. [23], we can deduce that here $\hat{m}_{\delta\phi}$ and T_{rh} gain almost their maximal allowed values since r_\pm is also maximized due to the hypothesis of Eq. (28). As a consequence, $m_{3/2}$ also has to be enhanced to avoid problems with BBN, whereas $m_{1,2D}$ and $M_{1,2N^c}$ are also constrained to larger values. On the other hand, our results are closer to those obtained employing the model of IG in Ref. [3] with gauge singlet inflaton and without unification constraint.

IV. CONCLUSIONS

We have proposed a class of novel inflationary models, referred to as IGHI, in which a Higgs field plays the role of the inflaton, before settling in its final vacuum state where it generates the Planck scale and gives rise to a mass for the gauge boson consistent with gauge coupling unification within MSSM. These two hypotheses allow us to determine (i) the mass scale M entering the superpotential in Eq. (1), and (ii) the quantity $r_\pm = c_+/c_-$ which expresses the amount of violation of a shift symmetry otherwise respected by the Kähler potentials considered in Eqs. (3a) – (3c). As a consequence, the inflationary scenario depends essentially on two free parameters (n and λ/c_-), leading naturally to observationally acceptable results. As an example, for $K = K_2$ or K_3 , $n = 0$ and $\lambda/c_- = 3 \cdot 10^{-5}$, we obtained $n_s \simeq 0.973$ and $r \simeq 0.0066$ with negligibly small a_s . Imposing a lower bound on c_- , we succeeded in implementing IGHI for subplanckian values of the inflaton, thereby stabilizing our predictions from possible higher order corrections in the super- and/or Kähler potentials. Moreover, the corresponding effective theory remains trustable up to m_P .

The models were further extended to generate the MSSM μ parameter, consistently with the low energy phenomenology. Successful baryogenesis is achieved via primordial leptogenesis, in agreement with the data on neutrino masses and mixing. More specifically, our post-inflationary setting favors the A/H funnel and the $\tilde{\chi}_1^\pm - \chi$ coannihilation regions of CMSSM with gravitino heavier than 10 TeV or so. Moreover, leptogenesis is realized through the out-of-equilibrium decay of the inflaton to the right-handed neutrinos N_1^c and/or N_2^c , with masses lower than $3.5 \cdot 10^{13}$ GeV, and a reheat temperature T_{rh} close to 10^9 GeV.

ACKNOWLEDGMENTS

C.P. acknowledges the Bartol Research Institute and the Department of Physics and Astronomy of the University of Delaware for its warm hospitality, during which this work has been initiated. He also acknowledges useful discussions with G. Lazarides and S. Martin. Q.S. acknowledges support by the DOE grant No. DE-SC0013880.

APPENDIX A: REMOVING THE INDEPENDENT KINETIC MIXING

Given that the necessary ingredient for the implementation of IGHI is just a convenient non-minimal coupling to gravity – see, e.g., Eqs. (16) and (28) –, the concerned reader could ask whether we can implement IGHI in a more minimal way, i.e., without the introduction of an independent kinetic mixing. This Appendix is devoted to this question. The relevant setting is presented in Sec. A 1, and the investigation of the inflationary and post-inflationary eras is displayed in Secs. A 2 and A 3 respectively. Some conclusions are given in Sec. A 4.

The Planck scale m_P is taken equal to unity in Secs. A 1, A 2 and A 4 and restored in Sec. A 3.

1. SET-UP

The aim of this Appendix is to check if we can attain inflationary solutions consistent with IG and unification constraints, combining W_{HI} in Eq. (1) with one of the following Kähler potentials

$$K_{1\mathcal{R}} = -N \ln \left(c_{\mathcal{R}} (\bar{\Phi}\Phi + \bar{\Phi}^*\Phi^*) - \frac{|\Phi|^2 + |\bar{\Phi}|^2}{N} + F_{1S} \right), \quad (\text{A1a})$$

which is completely logarithmic, and

$$K_{2\mathcal{R}} = -N \ln \left(c_{\mathcal{R}} (\bar{\Phi}\Phi + \bar{\Phi}^*\Phi^*) - \frac{|\Phi|^2 + |\bar{\Phi}|^2}{N} \right) + F_{2S}, \quad (\text{A1b})$$

which is polylogarithmic. Along the track in Eq. (18) and using the parametrization in Eq. (17), the non-minimal coupling to gravity, defined in Eq. (7) and induced by the K 's above read

$$f_{\mathcal{R}} = \frac{Nc_{\mathcal{R}} - 1}{2N} \phi^2. \quad (\text{A2})$$

The choice $K = K_{1\mathcal{R}}$ for $N = 3$, well-known from Ref. [19, 46], ensures canonical kinetic terms, whereas in the remaining cases a $c_{\mathcal{R}}$ -dependent kinetic mixing emerges, as can be easily shown by inserting the K 's above into Eq. (7) and computing the expression in the parenthesis of the second line in Eq. (8a). Indeed, in any case we have $\Omega_{\alpha\bar{\beta}} = \delta_{\alpha\bar{\beta}}$ and for $N = 3$ the second term in the parenthesis vanishes. Moving to EF we find always a $c_{\mathcal{R}}$ -dependent mixing expressed by the metric $K_{\alpha\bar{\beta}}$ which, along the path in Eq. (18), has the form in Eq. (23) with

$$M_{\pm} = \begin{pmatrix} (1 + Nc_{\mathcal{R}})/2f_{\mathcal{R}} & N/\phi^2 \\ N/\phi^2 & (1 + Nc_{\mathcal{R}})/2f_{\mathcal{R}} \end{pmatrix}. \quad (\text{A3})$$

Upon diagonalization of M_{\pm} we find the following eigenvalues

$$\kappa_+ = Nc_{\mathcal{R}}f_{\mathcal{R}}^{-1} \quad \text{and} \quad \kappa_- = f_{\mathcal{R}}^{-1}, \quad (\text{A4})$$

and so, we are not obliged to impose any condition here as in Eq. (25). Substituting κ_{\pm} into Eq. (26a) we derive the canonically normalized fields. The existence of the real function $|\Phi|^2 + |\bar{\Phi}|^2$ inside the argument of logarithm is vital for our scenario, since otherwise M_{\pm} develops zero eigenvalue and so it is singular, i.e., no $K^{\alpha\bar{\beta}}$ can be defined.

Therefore, the models employing the K 's in Eqs. (A1a) and (A1b) are more economical – and so deserve some attention – compared to the models based on the K 's in Eqs. (3a) – (3c). Indeed, the latter include two parameters (c_+ and c_-) from which one (c_+) enters $f_{\mathcal{R}}$ and the other (c_-) dominates independently the kinetic mixing. However, these parameters are related to a shift symmetry which renders the relevant setting theoretically more appealing.

2. INFLATIONARY ERA

Working along the lines of Sec. II A 2, we can confirm that the SUSY vacuum for the models considered in this Appendix lies along the direction in Eqs. (15) and (52). Combining Eqs. (15) and (16) we infer that the IG condition is now translated as

$$M = \sqrt{\frac{2N}{Nc_{\mathcal{R}} - 1}}. \quad (\text{A5})$$

Furthermore, along the track in Eq. (18), \hat{V} in Eq. (6b) takes the form shown in Eq. (19b) doing the replacements

$$f_W = (Nc_{\mathcal{R}} - 1)\phi^2 - 2N \quad \text{and} \quad c_+ = (Nc_{\mathcal{R}} - 1), \quad (\text{A6})$$

since again $K^{SS^*} = f_{\mathcal{R}} [K^{SS^*} = 1]$ for $K = K_{1\mathcal{R}}$ [$K = K_{2\mathcal{R}}$]. If we introduce from Eq. (19d) n defined for $K = K_{1\mathcal{R}}$ as for $K = K_1$ and for $K = K_{2\mathcal{R}}$ as for $K = K_2$ or K_3 , we can again obtain the universal expression in Eq. (20) employing Eqs. (A6) and (A2). For n close to zero, \hat{V}_{HI} is of Starobinsky type developing for $n > 0$ a local maximum given by Eq. (21) if c_+ is replaced by $c_{\mathcal{R}}/2$.

To consolidate the establishment of IGHI in this setting we derive the mass-squared spectrum of the $S - \Phi - \bar{\Phi}$ sector along the track in Eq. (18). This is shown in Table VI, from which we can verify the stability of the relevant fields and specify the gauge unification condition applying Eq. (27). In fact, we now obtain

$$c_{\mathcal{R}} = \frac{1}{N} + \frac{2g^2}{M_{\text{GUT}}^2} \simeq 1.451 \cdot 10^4, \quad (\text{A7})$$

leading to $M \simeq 0.0117$ via Eq. (A5). It is remarkable that here $c_{\mathcal{R}}$ is completely determined whereas Eq. (28) fixes just the ratio r_{\pm} . Although $c_{\mathcal{R}}$ above is very large, there is no problem with the validity of the effective theory, in accordance with the results of earlier works [3, 5, 11] on IG inflation with gauge singlet inflaton. Indeed, adapting the expansions in Eqs. (37a) and (37b) in our present case, we end up with the expressions

$$J^2 \dot{\phi}^2 \simeq \left(1 - \sqrt{\frac{2}{N}} \widehat{\delta\phi} + \frac{3}{2N} \widehat{\delta\phi}^2 - \sqrt{\frac{2}{N^3}} \widehat{\delta\phi}^3 + \dots \right) \widehat{\delta\phi}^2, \quad (\text{A8a})$$

and

$$\widehat{V}_{\text{HI}} \simeq \frac{\lambda^2 \widehat{\delta\phi}^2}{2c_{\mathcal{R}}^2} \left(1 - \frac{2N-1}{\sqrt{2N}} \widehat{\delta\phi} + \frac{8N^2-4N+1}{8N} \widehat{\delta\phi}^2 + \dots \right) \quad (\text{A8b})$$

which indicate that $\Lambda_{\text{UV}} = m_P$, since $c_{\mathcal{R}}$ does not appear in any of the numerators above.

Working along the lines of Sec. II C 2 we can investigate the inflationary dynamics estimating the slow-roll parameters as follows

$$\widehat{\epsilon} = 4 \frac{\tilde{f}_W^2 (n\tilde{f}_W - 2)^2}{Nc_{\mathcal{R}}^4 \phi^8} \quad \text{and} \quad \widehat{\eta} = 8 \frac{2 - \tilde{f}_W - 4n\tilde{f}_W + n^2\tilde{f}_W^2}{N\tilde{f}_W^2}, \quad (\text{A9})$$

TABLE VI: Mass-squared spectrum for $K = K_{1\mathcal{R}}$ and $K_{2\mathcal{R}}$ along the path in Eqs. (18) and (49).

FIELDS	EIGEN-STATES	MASSES SQUARED		
			$K = K_{1\mathcal{R}}$	$K = K_{2\mathcal{R}}$
14 Real Scalars	$\hat{\theta}_+$	$\hat{m}_{\theta_+}^2$	$6\hat{H}_{\text{HI}}^2(1 - 1/N)$	$6\hat{H}_{\text{HI}}^2$
	$\hat{\theta}_\Phi$	$\hat{m}_{\theta_\Phi}^2$	$M_{BL}^2 + 6\hat{H}_{\text{HI}}^2 c_{\mathcal{R}}(N - 3)$	$M_{BL}^2 + 6\hat{H}_{\text{HI}}^2 c_{\mathcal{R}}(N - 2)$
	$\hat{s}, \hat{\bar{s}}$	\hat{m}_s^2	$3\hat{H}_{\text{HI}}^2(N - 6 + c_{\mathcal{R}}\phi^2/N)$	$3\hat{H}_{\text{HI}}^2(4/N - 4 + N + 2/N_X)$
	$\hat{h}_\pm, \hat{\bar{h}}_\pm$	$\hat{m}_{h_\pm}^2$	$3\hat{H}_{\text{HI}}^2 c_{\mathcal{R}}(\phi^2/2N \pm 2\lambda_\mu/\lambda)$	$3\hat{H}_{\text{HI}}^2(1 + 1/N_X \pm 4\lambda_\mu/\lambda\phi^2)$
	$\hat{\nu}_i^c, \hat{\bar{\nu}}_i^c$	$\hat{m}_{\nu^c}^2$	$3\hat{H}_{\text{HI}}^2 c_{\mathcal{R}}(\phi^2/2N + 8\lambda_{iN^c}^2/\lambda^2)$	$3\hat{H}_{\text{HI}}^2(1 + 1/N_X + 16\lambda_{iN^c}^2/\lambda^2\phi^2)$
1 Gauge Boson	A_{BL}	M_{BL}^2	$2Ng^2/(Nc_{\mathcal{R}} - 1)$	
7 Weyl Spinors	$\hat{\psi}_\pm$	$\hat{m}_{\psi_\pm}^2$	$3\hat{H}_{\text{HI}}^2(c_{\mathcal{R}}(N - 2)\phi^2 - 2N)^2/N^2 c_{\mathcal{R}}^2\phi^4$	
	$\lambda_{BL}, \hat{\psi}_{\Phi-}$	M_{BL}^2	$2Ng^2/(Nc_{\mathcal{R}} - 1)$	
	\hat{N}_i^c	$\hat{m}_{iN^c}^2$	$48\hat{H}_{\text{HI}}^2 c_{\mathcal{R}}\lambda_{iN^c}^2/\lambda^2\phi^2$	

where $\tilde{f}_W = c_{\mathcal{R}}\phi^2 - 2$. The condition Eq. (29a) is violated for $\phi = \phi_f$, which is found to be

$$\phi_f \simeq \max \left(\frac{2}{\sqrt{c_{\mathcal{R}}}} \sqrt{\frac{1+n}{2n+\sqrt{N}}}, 2\sqrt{\frac{2}{c_{\mathcal{R}}}} \sqrt{\frac{1-4n}{8n^2+N}} \right). \quad (\text{A10})$$

Then, \hat{N}_* can be also computed from Eq. (32) as follows

$$\hat{N}_* \simeq \begin{cases} Nc_{\mathcal{R}}\phi_*^2/8 & \text{for } n = 0, \\ N \ln \left(\frac{2(1+n)}{2-n\tilde{f}_{W*}} \right) / 4n(1+n) & \text{for } n \neq 0, \end{cases} \quad (\text{A11})$$

where $\tilde{f}_{W*} = \tilde{f}_W(\hat{\phi}_*)$. Solving the above equations w.r.t ϕ_* we obtain a unified expression

$$\phi_* \simeq \sqrt{\frac{2f_{\mathcal{R}*}}{c_{\mathcal{R}}}} \quad \text{with} \quad f_{\mathcal{R}*} = \frac{1+n}{n} \left(1 - e^{-4n(1+n)\hat{N}_*/N} \right) \quad (\text{A12})$$

reducing to $4\hat{N}_*/N$ in the limit $n \rightarrow 0$. For $c_{\mathcal{R}}$ in Eq. (A7) we can verify that $\phi_* \sim 0.1$ and so the model is (automatically) well stabilized against corrections from higher order terms. On the contrary, Eq. (36) is imposed by hand. Thanks to Eq. (A7), we can derive uniquely λ from the expression

$$\lambda = 8\sqrt{6A_s\pi c_{\mathcal{R}} f_{\mathcal{R}*}^{n+1}} \frac{n(1-f_{\mathcal{R}*})+1}{\sqrt{N}(f_{\mathcal{R}*}-1)^2}, \quad (\text{A13})$$

applying the second equation in Eq. (32). As n varies in its allowed ranges presented below, we obtain

$$2.3 \lesssim \lambda/0.1 \lesssim 4 \quad \text{or} \quad 1.9 \lesssim \lambda/0.1 \lesssim 3.5, \quad (\text{A14})$$

for $K = K_{1\mathcal{R}}$ or $K = K_{2\mathcal{R}}$ respectively. If we take $n = 0$, we find the central values of λ in the ranges above which are 0.29 and 0.24 correspondingly.

Upon substitution of $f_{\mathcal{R}*}$ into Eq. (39a) we obtain the predictions of the model which are

$$n_s \simeq 1 - \frac{8n^2}{N} + \frac{16}{N} \frac{n}{f_{\mathcal{R}*}-1} - \frac{8}{N} \frac{f_{\mathcal{R}*}+1}{(f_{\mathcal{R}*}-1)^2}, \quad (\text{A15a})$$

$$r \simeq \frac{64}{N} \left(\frac{1+n(1-f_{\mathcal{R}*})}{f_{\mathcal{R}*}-1} \right)^2, \quad (\text{A15b})$$

where we can recognize the similarities with the formulas given in Eqs. (39a) and (40b). Since only $|n| \ll 1$ are allowed, as we see below, the results above, together with a_s , can be further simplified as follows

$$n_s \simeq 1 - \frac{2}{\hat{N}_*} - \frac{4n}{N} - \frac{8n^2\hat{N}_*}{3N^2}, \quad (\text{A16a})$$

$$r \simeq \frac{4N}{\hat{N}_*^2} - \frac{16n^3}{N} + \frac{80n^2}{3N} - \frac{64n^3\hat{N}_*}{3N^2}, \quad (\text{A16b})$$

$$a_s \simeq -\frac{2}{\hat{N}_*^2} + \frac{3n}{\hat{N}_*^2} + \frac{8n^2}{3N^2} - \frac{7N}{2\hat{N}_*^3}, \quad (\text{A16c})$$

where, for $n = 0$, the well-known predictions of the Starobinsky model are recovered, i.e., $n_s \simeq 0.966$ and $r = 0.0032$ [$r = 0.0022$] for $K = K_{1\mathcal{R}}$ [$K = K_{2\mathcal{R}}$]. On the other hand, contributions proportional to \hat{N}_* can be tamed for sufficiently low n as we can verify numerically.

Indeed, in Fig. 6 we depict by a dashed [solid] line the model predictions for $K = K_{1\mathcal{R}}$ [$K = K_{2\mathcal{R}}$] against the observational data. We see that the whole observationally favored range at low r 's is covered as in Fig. 1. We remark, though, that n remains closer to zero and r is slightly lower compared to that obtained in Sec. II C 2. More explicitly, we find the allowed ranges

$$0.9 \gtrsim n/0.01 \gtrsim -1 \quad \text{and} \quad 1.5 \lesssim r/10^{-3} \lesssim 6.6 \quad (\text{A17a})$$

for $K = K_{1\mathcal{R}}$, whereas for $K = K_{2\mathcal{R}}$ we have

$$5.1 \gtrsim n/0.001 \gtrsim -9 \quad \text{and} \quad 1.1 \lesssim r/10^{-3} \lesssim 5.9. \quad (\text{A17b})$$

No observationally acceptable attractor to linear inflation [54] is detected here.

3. POST-INFLATIONARY ERA

To proceed further, we consider the completion described in Sec. III A. For this reason we arrange in Table VI the excitations of the fields involved in Eqs. (48a) and (48b) along

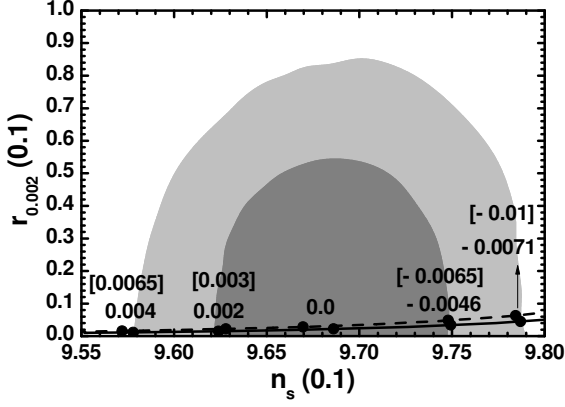


FIG. 6: Same as Fig. 1 but for $K = K_{1\mathcal{R}}$ (dashed line) and $K = K_{2\mathcal{R}}$ (solid line) – the n values in [outside] squared brackets correspond to $K = K_{1\mathcal{R}}$ [$K = K_{2\mathcal{R}}$].

the path in Eqs. (18) and (49). From the results there we can remark that assuring $\widehat{m}_{h^-}^2 > 0$ dictates again a condition on λ_μ . Namely, we obtain

$$\lambda_\mu \lesssim \lambda\phi^2/4N \quad \text{for } K = K_{1\mathcal{R}}; \quad (\text{A18a})$$

$$\lambda_\mu \lesssim \lambda\phi^2(1 + 1/N_X)/4 \quad \text{for } K = K_{2\mathcal{R}}, \quad (\text{A18b})$$

which are again fulfilled for $\lambda_\mu \lesssim 2 \cdot 10^{-5}$.

Under this condition, the generation of μ term can be processed following the steps described in Sec. III B 1. Namely, we compute V_{tot} in Eq. (54) with all the fields except S equal to their v.e.vs in Eqs. (15) and (52). The result is

$$\langle V_{\text{tot}}(S) \rangle = \frac{\lambda^2 m_{\text{P}}^2 S^2}{c_{\mathcal{R}}(N c_{\mathcal{R}} - 1)} - \lambda a_{3/2} m_{3/2} M^2 S. \quad (\text{A19a})$$

The minimization of $\langle V_{\text{tot}}(S) \rangle$ w.r.t S leads to a new non vanishing $\langle S \rangle$,

$$\langle S \rangle \simeq N a_{3/2} m_{3/2} c_{\mathcal{R}} / \lambda, \quad (\text{A19b})$$

where M is replaced by Eq. (A5). Therefore, the μ parameter involved in Eq. (48b) is

$$\mu = \lambda_\mu \langle S \rangle = N \lambda_\mu a_{3/2} m_{3/2} c_{\mathcal{R}} / \lambda. \quad (\text{A19c})$$

This still depends only n thanks to the condition in Eq. (A13) which fixes $\lambda/c_{\mathcal{R}}$ as a function of n – see Eq. (A12).

Repeating the procedure outlined in Sec. III B 2 we find the λ_μ values, listed in Table VII, which are compatible with the best-fit points of CMSSM for $n = 0$. These λ_μ values are lower than those listed in Table IV, larger than those found in Ref. [23], and similar to those in Ref. [3] especially for $K = K_{1\mathcal{R}}$. Checking if these λ_μ values are in accord with the conditions Eqs. (A18a) and (A18b), we infer that these inequalities are violated in $\tilde{\tau}_1 - \chi$ coannihilation region for $K = K_{1\mathcal{R}}$, and are fulfilled for $K = K_{2\mathcal{R}}$ only by setting $N_X \leq 1.2$, similarly to the findings in Sec. III B 2. The CMSSM regions favored by the \tilde{G} constraint are the same as those mentioned there.

TABLE VII: Same as Table IV but for $K = K_{1\mathcal{R}}$ and $K_{2\mathcal{R}}$.

CMSSM REGION:	A/H FUNNEL	COANNIHILATION		
		$\tilde{\tau}_1 - \chi$	$\tilde{t}_1 - \chi$	$\tilde{\chi}_1^\pm - \chi$
$\lambda_\mu(10^{-6})$ for $K = K_{1\mathcal{R}}$				
$n = 0$	0.963	14.48	2.91	0.723
$\lambda_\mu(10^{-6})$ for $K = K_{2\mathcal{R}}$				
$n = 0$	1.184	17.81	3.41	0.89

TABLE VIII: Same as in Table V but for $K = K_{2\mathcal{R}}$ and $n = 0$.

PARAMETERS	CASES						
	A	B	C	D	E	F	G
Low Scale Parameters as in Table V							
Leptogenesis-Scale Mass Parameters in GeV							
$m_{iD}^{(*)}$	1.91	16.6	11.6	10.15	9.25	6.37	9.5
(*) Where $i = 1$ for case A and $i = 2$ for the others.							
The remaining m_{iD} and M_{iN^c} are as in Table V.							
Resulting B -Yield							
$Y_B^0/10^{-11}$	9.6	7.8	8.5	8.9	8.9	8.9	8.7
$Y_B/10^{-11}$	8.64	8.61	8.72	8.6	8.73	8.8	8.5
Resulting T_{rh} (in GeV) and \tilde{G} -Yield							
$T_{\text{rh}}/10^8$	7.6	8.4	7.7	8.4	7.6	7.6	7.8
$Y_{3/2}/10^{-13}$	1.44	2.9	1.5	1.6	1.45	1.45	1.5

At the SUSY vacuum in Eqs. (15) and (52), the mass of the inflaton $\widehat{\delta\phi}$ in Eq. (58) with $\langle J \rangle = \sqrt{N c_{\mathcal{R}}}$ is given by

$$\widehat{m}_{\delta\phi} = \frac{\lambda m_{\text{P}}}{\sqrt{c_{\mathcal{R}}(N c_{\mathcal{R}} - 1)}}. \quad (\text{A20})$$

From the last expression we can infer that $\widehat{m}_{\delta\phi}$ remains constant for fixed n since $\lambda/c_{\mathcal{R}}$ is fixed too – see Eq. (A13). More specifically, for the allowed range of n in Eqs. (A17a) and (A17b) we obtain

$$2. \lesssim \widehat{m}_{\delta\phi}/10^{13} \text{ GeV} \lesssim 3.9 \quad \text{for } K = K_{1\mathcal{R}}, \quad (\text{A21a})$$

$$2.1 \lesssim \widehat{m}_{\delta\phi}/10^{13} \text{ GeV} \lesssim 4.5 \quad \text{for } K = K_{2\mathcal{R}}, \quad (\text{A21b})$$

with the value $\widehat{m}_{\delta\phi} = 2.8 \cdot 10^{13} \text{ GeV}$ corresponding to $n = 0$. The decay of $\widehat{\delta\phi}$ proceeds via the channels quoted in Sec. III C 1 with decay widths given by Eqs. (62a), (63a) and (64a), where g_{iN^c} is given by the first equation in Eq. (62b) with $\langle J \rangle = \sqrt{N c_{\mathcal{R}}}$, g_H remains unaltered, while g_y reads

$$g_y = y_3 \left(\frac{N c_{\mathcal{R}} - 1}{2 c_{\mathcal{R}}} \right)^{1/2}. \quad (\text{A22})$$

Applying, finally, the approach described in Sec. III C 3, we can examine if nTL can be successfully implemented. To accomplish this we construct Table VIII taking $K = K_{2\mathcal{R}}$ with

$n = 0$ and employing the low energy neutrino spectra shown in Table V. Adjusting m_{1D} in case A or m_{2D} in the other cases we can again accommodate Y_B within the range of Eq. (67) keeping the remaining m_{iD} unchanged. As a consequence, M_{iN^c} deviate very little from the values shown in Table V with the resulting T_{rh} and $Y_{3/2}$ being a little lower than those found there. The $m_{3/2}$'s dictated by Eq. (71), though, must still be large enough and of the order of 10 TeV. Had we employed $K = K_{2\mathcal{R}}$, we would have obtained almost two times larger Y_B values since g_{iN^c} depends on N , which is larger ($N = 3$) for $K = K_{1\mathcal{R}}$ than for $K = K_{2\mathcal{R}}$ ($N = 2$).

4. CONCLUDING REMARKS

Recapitulating this Appendix, we can say that the models based on K 's in Eqs. (A1a) and (A1b) yield results similar to the ones obtained employing the K 's in Eqs. (3a) – (3c). The former group of K 's have the advantage that they are more economical and lead to slightly lower T_{rh} 's. On the other hand, the latter exhibit a softly broken shift symmetry, lead to slightly larger r 's and yield two distinct allowed regions of parameters with n values one order of magnitude larger than those needed for $K = K_{1\mathcal{R}}$ and $K_{2\mathcal{R}}$. For $K = K_2$ and K_3 the generation of the μ term is technically simpler since F_{1S}

with $l = 2, 3$ is placed outside the logarithm with coefficient ($-N$) and no expansion in powers $1/m_P$ is necessitated. In all cases the effective theories are valid up-to m_P .

Another possibility that could be inspected is what happens if we place the term $c_- F_-$ inside the argument of the logarithm in Eqs. (3a) and (3b) – cf. Ref. [20] – considering the Kähler potentials

$$K_{01} = -N \ln(c_+ F_+ - c_- F_- / N + F_{1S}), \quad (\text{A23a})$$

$$K_{02} = -N \ln(c_+ F_+ - c_- F_- / N) + F_{2S}. \quad (\text{A23b})$$

These K 's, though, reduce to $K_{1\mathcal{R}}$ and $K_{2\mathcal{R}}$ respectively if we set

$$c_+ = \frac{Nc_{\mathcal{R}} - 1}{2N} \quad \text{and} \quad c_- = \frac{Nc_{\mathcal{R}} + 1}{2}. \quad (\text{A24})$$

For $c_{\mathcal{R}} \gg 1$ the arrangement above results in $r_{\pm} \simeq 1/N$. On the other hand, the same r_{\pm} is found if we derive $\langle M_{BL} \rangle$ and extract r_{\pm} via Eq. (28). Therefore, the observational predictions of the models based on the K 's above are expected to be very similar to those obtained using Eqs. (A1a) and (A1b) and depicted in Fig. 6. This conclusion may be verified by direct computation.

REFERENCES

- [1] A. Zee, *Phys. Rev. Lett.* **42**, 417 (1979); H. Terazawa, *Phys. Lett. B* **101**, 43 (1981).
- [2] A.A. Starobinsky, *Phys. Lett. B* **91**, 99 (1980).
- [3] C. Pallis, *J. Cosmol. Astropart. Phys.* **04**, 024 (2014); **07**, 01(E) (2017) [arXiv:1312.3623].
- [4] R. Kallosh, *Phys. Rev. D* **89**, 087703 (2014) [arXiv:1402.3286].
- [5] C. Pallis, *J. Cosmol. Astropart. Phys.* **08**, 057 (2014) [arXiv:1403.5486]; C. Pallis, *J. Cosmol. Astropart. Phys.* **10**, 058 (2014) [arXiv:1407.8522]; C. Pallis, *PoS CORFU 2014*, 156 (2015) [arXiv:1506.03731].
- [6] C. Pallis and N. Toumbas, *J. Cosmol. Astropart. Phys.* **05**, no. 05, 015 (2016) [arXiv:1512.05657]; C. Pallis and N. Toumbas, *Adv. High Energy Phys.* **2017**, 6759267 (2017) [arXiv:1612.09202]; C. Pallis, *PoS EPS-HEP 2017*, 047 (2017) [arXiv:1710.04641].
- [7] M.B. Einhorn and D.R.T. Jones, *J. Cosmol. Astropart. Phys.* **11**, 049 (2012) [arXiv:1207.1710].
- [8] F.S. Accetta, D.J. Zoller, and M.S. Turner, *Phys. Rev. D* **31**, 3046 (1985); R. Fakir and W.G. Unruh, *Phys. Rev. D* **41**, 1792 (1990); D.I. Kaiser, *Phys. Rev. D* **52**, 4295 (1995) [astro-ph/9408044].
- [9] D.S. Salopek, J.R. Bond and J.M. Bardeen, *Phys. Rev. D* **40**, 1753 (1989); J.L. Cervantes-Cota and H. Dehnen, *Phys. Rev. D* **51**, 395 (1995) [astro-ph/9412032].
- [10] N. Kaloper, L. Sorbo and J. Yokoyama, *Phys. Rev. D* **78**, 043527 (2008) [arXiv:0803.3809].
- [11] G.F. Giudice and H.M. Lee, *Phys. Lett. B* **733**, 58 (2014) [arXiv:1402.2129].
- [12] K. Kannike *et al.*, *J. High Energy Phys.* **05**, 065 (2015) [arXiv:1502.01334]; M.B. Einhorn and D.R.T. Jones, *J. High Energy Phys.* **01**, 019 (2016) [arXiv:1511.01481].
- [13] P.A.R. Ade *et al.* [Planck Collaboration], *Astron. Astrophys.* **594**, A20 (2016) [arXiv:1502.02114].
- [14] J.L.F. Barbon and J.R. Espinosa, *Phys. Rev. D* **79**, 081302 (2009) [arXiv:0903.0355]; C.P. Burgess, H.M. Lee and M. Trott, *J. High Energy Phys.* **07**, 007 (2010) [arXiv:1002.2730].
- [15] A. Kehagias, A.M. Dizgah and A. Riotto, *Phys. Rev. D* **89**, 043527 (2014) [arXiv:1312.1155].
- [16] C. Pallis, *Phys. Lett. B* **692**, 287 (2010) [arXiv:1002.4765].
- [17] R. Kallosh, A. Linde and D. Roest, *Phys. Rev. Lett.* **112**, 011303 (2014) [arXiv:1310.3950].
- [18] N. Okada, M.U. Rehman, and Q. Shafi, *Phys. Rev. D* **82**, 043502 (2010) [arXiv:1005.5161].
- [19] C. Pallis and N. Toumbas, *J. Cosmol. Astropart. Phys.* **12**, 002 (2011) [arXiv:1108.1771]; C. Pallis and N. Toumbas, “Open Questions in Cosmology” (InTech, 2012) [arXiv:1207.3730].
- [20] G. Lazarides and C. Pallis, *J. High Energy Phys.* **11**, 114 (2015) [arXiv:1508.06682].
- [21] C. Pallis, *Phys. Rev. D* **92**, no. 12, 121305(R) (2015) [arXiv:1511.01456].
- [22] C. Pallis, *J. Cosmol. Astropart. Phys.* **10**, no. 10, 037 (2016) [arXiv:1606.09607].
- [23] C. Pallis, *Universe* **4**, no. 1, 13 (2018) [arXiv:1510.05759].
- [24] G.R. Dvali, Q. Shafi and R.K. Schaefer, *Phys. Rev. Lett.* **73**, 1886 (1994) [hep-ph/9406319].
- [25] G.R. Dvali, G. Lazarides and Q. Shafi, *Phys. Lett. B* **424**, 259 (1998) [hep-ph/9710314].
- [26] M. Bastero-Gil, S.F. King and Q. Shafi, *Phys. Lett. B* **651**, 345 (2007) [hep-ph/0604198]; B. Garbrecht, C. Pal-

- lis and A. Pilaftsis, *J. High Energy Phys.* **12**, 038 (2006) [hep-ph/0605264]; M.U. Rehman, V.N. Şenoğuz and Q. Shafi, *Phys. Rev. D* **75**, 043522 (2007) [hep-ph/0612023]; C. Pallis, *J. Cosmol. Astropart. Phys.* **04**, 024 (2009) [arXiv:0902.0334]; M. Civeletti, C. Pallis and Q. Shafi, *Phys. Lett. B* **733**, 276 (2014) [arXiv:1402.6254].
- [27] V.N. Şenoğuz and Q. Shafi, hep-ph/0512170; W. Buchmüller, V. Domcke and K. Schmitz, *Nucl. Phys.* **B862**, 587 (2012) [arXiv:1202.6679]; C. Pallis and Q. Shafi, *Phys. Lett. B* **725**, 327 (2013) [arXiv:1304.5202].
- [28] N. Okada and Q. Shafi, *Phys. Lett. B* **775**, 348 (2017) [arXiv:1506.01410].
- [29] N. Okada and Q. Shafi, arXiv:1709.04610.
- [30] M. Kawasaki, M. Yamaguchi and T. Yanagida, *Phys. Rev. Lett.* **85**, 3572 (2000) [hep-ph/0004243]; P. Brax and J. Martin, *Phys. Rev. D* **72**, 023518 (2005) [hep-th/0504168]; S. Antusch, K. Dutta and P.M. Kostka, *Phys. Lett. B* **677**, 221 (2009) [arXiv:0902.2934]; R. Kallosh, A. Linde and T. Rube, *Phys. Rev. D* **83**, 043507 (2011) [arXiv:1011.5945]; T. Li, Z. Li and D.V. Nanopoulos, *J. Cosmol. Astropart. Phys.* **02**, 028 (2014) [arXiv:1311.6770]; K. Harigaya and T.T. Yanagida, *Phys. Lett. B* **734**, 13 (2014) [arXiv:1403.4729]; A. Mazumdar, T. Noumi and M. Yamaguchi, *Phys. Rev. D* **90**, 043519 (2014) [arXiv:1405.3959]; C. Pallis and Q. Shafi, *Phys. Lett. B* **736**, 261 (2014) [arXiv:1405.7645].
- [31] I. Ben-Dayan and M.B. Einhorn, *J. Cosmol. Astropart. Phys.* **12**, 002 (2010) [arXiv:1009.2276].
- [32] C. Pallis, *Phys. Rev. D* **91**, no. 12, 123508 (2015) [arXiv:1503.05887]; C. Pallis, *PoS PLANCK 2015*, 095 (2015) [arXiv:1510.02306].
- [33] P.A.R. Ade *et al.* [BICEP2/Keck Array Collaborations], *Phys. Rev. Lett.* **116**, 031302 (2016) [arXiv:1510.09217].
- [34] W.L.K. Wu *et al.*, *J. Low. Temp. Phys.* **184**, no. 3-4, 765 (2016) [arXiv:1601.00125].
- [35] P. Andre *et al.* [PRISM Collaboration], arXiv:1306.2259.
- [36] T. Matsumura *et al.*, *J. Low. Temp. Phys.* **176**, 733 (2014) [arXiv:1311.2847].
- [37] F. Finelli *et al.* [CORE Collaboration] arXiv:1612.08270.
- [38] K. Hamaguchi, *Phd Thesis* [hep-ph/0212305]; W. Buchmüller, R.D. Peccei and T. Yanagida, *Ann. Rev. Nucl. Part. Sci.* **55**, 311 (2005) [hep-ph/0502169].
- [39] G. Lazarides and Q. Shafi, *Phys. Lett. B* **258**, 305 (1991); K. Kumekawa, T. Moroi and T. Yanagida, *Prog. Theor. Phys.* **92**, 437 (1994) [hep-ph/9405337]; G. Lazarides, R.K. Schaefer and Q. Shafi, *Phys. Rev. D* **56**, 1324 (1997) [hep-ph/9608256]; V.N. Şenoğuz and Q. Shafi, *Phys. Rev. D* **71**, 043514 (2005) [hep-ph/0412102].
- [40] M.Yu. Khlopov and A.D. Linde, *Phys. Lett. B* **138**, 265 (1984); J. Ellis, J.E. Kim, and D.V. Nanopoulos, *Phys. Lett. B* **145**, 181 (1984).
- [41] M. Bolz, A.Brandenburg and W. Buchmüller, *Nucl. Phys.* **B606**, 518 (2001); **790**, 336(E) (2008) [hep-ph/0012052]; J. Pradler and F.D. Steffen, *Phys. Rev. D* **75**, 023509 (2007) [hep-ph/0608344].
- [42] M.Kawasaki, K.Kohri and T.Moroi, *Phys. Lett. B* **625**, 7 (2005) [astro-ph/0402490]; M. Kawasaki, K. Kohri and T. Moroi, *Phys. Rev. D* **71**, 083502 (2005) [astro-ph/0408426]; J.R. Ellis, K.A. Olive and E. Vangioni, *Phys. Lett. B* **619**, 30 (2005) [astro-ph/0503023]; M. Kawasaki, K. Kohri, T. Moroi and Y. Takaesu, *Phys. Rev. D* **97**, no. 2, 023502 (2018) [arXiv:1709.01211].
- [43] J. Ellis *et al.*, *J. Cosmol. Astropart. Phys.* **03**, no. 03, 008 (2016) [arXiv:1512.05701]; Y. Ema *et al.*, *J. High Energy Phys.* **11**, 184 (2016) [arXiv:1609.04716].
- [44] D.V. Forero, M. Tortola and J.W.F. Valle, *Phys. Rev. D* **90**, no. 9, 093006 (2014) [arXiv:1405.7540].
- [45] M.C. Gonzalez-Garcia, M. Maltoni and T. Schwetz, *J. High Energy Phys.* **11**, 052 (2014) [arXiv:1409.5439]; F. Capozzi *et al.*, *Nucl. Phys. B* **908**, 218 (2016) [arXiv:1601.07777].
- [46] M.B. Einhorn and D.R.T. Jones, *J. High Energy Phys.* **03**, 026 (2010) [arXiv:0912.2718]; H.M. Lee, *J. Cosmol. Astropart. Phys.* **08**, 003 (2010) [arXiv:1005.2735]; S. Ferrara *et al.*, *Phys. Rev. D* **83**, 025008 (2011) [arXiv:1008.2942]; C. Pallis and N. Toumbas, *J. Cosmol. Astropart. Phys.* **02**, 019 (2011) [arXiv:1101.0325].
- [47] G. Lopes Cardoso, D. Lust and T. Mohaupt, *Nucl. Phys.* **B432** 68 (1994) [hep-th/9405002]; I. Antoniadis, E. Gava, K.S. Narain and T.R. Taylor, *Nucl. Phys.* **B432** 187 (1994) [hep-th/9405024].
- [48] R. Kallosh, A. Linde and D. Roest, *J. High Energy Phys.* **11**, 198 (2013) [arXiv:1311.0472]; R. Kallosh, A. Linde and D. Roest, *J. High Energy Phys.* **08**, 052 (2014) [arXiv:1405.3646].
- [49] L. Boubekeur and D. Lyth, *J. Cosmol. Astropart. Phys.* **07**, 010 (2005) [hep-ph/0502047].
- [50] S.R. Coleman and E.J. Weinberg, *Phys. Rev. D* **7**, 1888 (1973).
- [51] D.H. Lyth and A. Riotto, *Phys. Rept.* **314**, 1 (1999) [hep-ph/9807278]; J. Martin, C. Ringeval and V. Vennin, *Physics of the Dark Universe* **5-6**, 75 (2014) [arXiv:1303.3787].
- [52] <http://functions.wolfram.com>.
- [53] P.A.R. Ade *et al.* [Planck Collaboration], *Astron. Astrophys.* **594**, A13 (2016) [arXiv:1502.01589].
- [54] A. Racioppi, arXiv:1801.08810.
- [55] G. Lazarides and Q. Shafi, *Phys. Rev. D* **58**, 071702 (1998) [hep-ph/9803397].
- [56] S. Antusch and M. Spinrath, *Phys. Rev. D* **78**, 075020 (2008) [arXiv:0804.0717].
- [57] W. Buchmüller *et al.*, *J. High Energy Phys.* **09**, 053 (2014) [arXiv:1407.0253]; J. Ellis, M. Garcia, D. Nanopoulos and K. Olive, *J. Cosmol. Astropart. Phys.* **10**, 003 (2015) [arXiv:1503.08867]; E. Dudas, T. Gherghetta, Y. Mambrini and K.A. Olive, *Phys. Rev. D* **96**, no. 11, 115032 (2017) [arXiv:1710.07341].
- [58] P. Athron *et al.* [GAMBIT Collaboration], *Eur. Phys. J. C* **77**, no. 12, 824 (2017) [arXiv:1705.07935].
- [59] M. Endo, F. Takahashi and T.T. Yanagida, *Phys. Rev. D* **76**, 083509 (2007) [arXiv:0706.0986].
- [60] C. Pallis, *Nucl. Phys.* **B751**, 129 (2006) [hep-ph/0510234].
- [61] S. Antusch, J. Kersten, M. Lindner and M. Ratz, *Nucl. Phys.* **B674**, 401 (2003) [hep-ph/0305273].
- [62] V.N. Şenoğuz, *Phys. Rev. D* **76**, 013005 (2007) [arXiv:0704.3048].
- [63] A. Gando *et al.* [KamLAND-Zen Collaboration], *Phys. Rev. Lett* **117**, no.8, 082503.(2016); *ibid* **17**, no.10, 109903 (2016).
- [64] N. Karagiannakis, G. Lazarides and C. Pallis, *Phys. Rev. D* **92**, no. 8, 085018 (2015) [arXiv:1503.06186].
- [65] H. Baer *et al.*, *Phys. Rev. Lett.* **109**, 161802 (2012) [arXiv:1207.3343].